

SPADE: Sequential-clustering Particle Annihilation via Discrepancy Estimation

Sihong Shao[†] Yunfeng Xiong[†]

December 22, 2024

Abstract

For an empirical signed measure $\mu = \frac{1}{N} \left(\sum_{i=1}^P \delta_{\mathbf{x}_i} - \sum_{i=1}^M \delta_{\mathbf{y}_i} \right)$, particle annihilation (PA) removes N_A particles from both $\{\mathbf{x}_i\}_{i=1}^P$ and $\{\mathbf{y}_i\}_{i=1}^M$ simultaneously, yielding another empirical signed measure ν such that $\int f d\nu$ approximates to $\int f d\mu$ within an acceptable accuracy for suitable test functions f . Such annihilation of particles carrying opposite importance weights has been extensively utilized for alleviating the numerical sign problem in particle simulations. In this paper, we propose an algorithm for PA in high-dimensional Euclidean space based on hybrid of clustering and matching, dubbed the Sequential-clustering Particle Annihilation via Discrepancy Estimation (SPADE). It consists of two steps: Adaptive clustering of particles via controlling their number-theoretic discrepancies, and independent random matching among positive and negative particles in each cluster. Both deterministic error bounds by the Koksma-Hlawka inequality and non-asymptotic random error bounds by concentration inequalities are proved to be affected by two factors. One factor measures the irregularity of point distributions and reflects their discrete nature. The other relies on the variation of test function and is influenced by the continuity. Only the latter implicitly depends on dimensionality d , implying that SPADE can be immune to the curse of dimensionality for a wide class of test functions. Numerical experiments up to $d = 1080$ validate our theoretical discoveries.

AMS subject classifications: 62G09; 11K38; 65D40; 62G07; 62D05

Keywords: Particle annihilation; Signed measure; Discrepancy; Concentration inequality; Density estimation

[†]LMAM and School of Mathematical Sciences, Peking University, Beijing 100871, China. Email addresses: sihong@math.pku.edu.cn (S. Shao), xiongyf1990@pku.edu.cn (Y. Xiong).

Contents

1	Introduction	2
2	Notations and definitions	5
3	Statement of main theorems	7
4	Clustering and discrepancy theory	9
4.1	Setting of sequential clustering	10
4.2	Deterministic bounds under arbitrary matching	12
5	Matching and concentration inequalities	15
5.1	Stochastic bounds under random matching	16
5.2	Variance estimation via bounding discrepancies	19
6	Numerical validation	23
6.1	Experiment setup	24
6.2	Implementation	25
6.3	Numerical results	26
7	Conclusion and discussion	27
8	Supplementary: Raw data in numerical experiments	32

1 Introduction

Given two sequences $\mathcal{X} = (\mathbf{x}_1, \dots, \mathbf{x}_P) \subset \mathbb{Q}^P$ and $\mathcal{Y} = (\mathbf{y}_1, \dots, \mathbf{y}_M) \subset \mathbb{Q}^M$ in a finite rectangular domain $\mathbb{Q} \subset \mathbb{R}^d$, \mathcal{X} and \mathcal{Y} are sets of positive and negative particles, carrying opposite weights 1 and -1 , respectively. An empirical signed measure μ is given by

$$\mu = \frac{1}{N} \left(\sum_{i=1}^P \delta_{\mathbf{x}_i} - \sum_{i=1}^M \delta_{\mathbf{y}_i} \right), \quad (1.1)$$

where $N > 0$ is a prescribed normalizing constant and $\delta_{\mathbf{x}}$ is Dirac measure concentrated at \mathbf{x} . Typical choices of N include $N = N_{tot}$ with $N_{tot} = P + M$ the total particle number or $N = P - M$ for $P > M$ in order to make $\mu(\mathbb{Q}) = 1$. Removing N_A positive particles from \mathcal{X} and N_A negative ones from \mathcal{Y} simultaneously yields two subsets $\mathcal{X}^A = (\tilde{\mathbf{x}}_1, \dots, \tilde{\mathbf{x}}_{P-N_A}) \subset \mathcal{X}$ and $\mathcal{Y}^A = (\tilde{\mathbf{y}}_1, \dots, \tilde{\mathbf{y}}_{M-N_A}) \subset \mathcal{Y}$ and another empirical signed measure

$$\nu = \frac{1}{N} \left(\sum_{i=1}^{P-N_A} \delta_{\tilde{\mathbf{x}}_i} - \sum_{i=1}^{M-N_A} \delta_{\tilde{\mathbf{y}}_i} \right). \quad (1.2)$$

Of direct interest in various applications is seeking a strategy to diminish the error function

$$\mathcal{E}(f) = \int f(d\mu - d\nu) \quad (1.3)$$

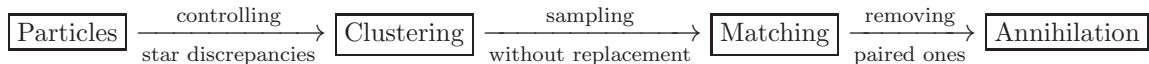
for a suitable class of test functions f .

The aforementioned problem is called particle annihilation (PA) since positive and negative particles are paired and annihilated, so that the opposite importance weights are cancelled out. It is also known as particle cancelation or particle resampling on some occasions. PA is originated from a vast number of Monte Carlo applications ranging from classical particle transport to quantum Monte Carlo. In classical regime, the signed measure describes fluctuations over the equilibrium.^{1,33} While in quantum mechanics, negative weights emerge in Monte Carlo integration of oscillatory and determinantal functions, including the path-integral representation of quantum observables,⁴ the pseudo-differential operator in the Wigner dynamics^{13,25} and the Rayleigh quotients with Slater determinant ansatz of fermionic wave-functions.²²

Unfortunately, stochastic estimators of the form in Eq. (1.1) usually suffer from the notorious numerical sign problem due to the near-cancelation of contributions from positive and negative weights, which stem from oscillating functions or even and odd permutations in determinants.⁹ As a consequence, it leads to an exponential increase of particle number and stochastic variance, as well as the computational complexity, especially when simulating long-time particle dynamics.^{4,22,25,33} The sign problem is believed to be NP-hard since there might not exist an algorithm to achieve a relative statistical error scaling polynomially with the dimensionality d and the system size in general.^{12,30} A well-known example is given in³⁰ by mapping a 3-D Ising spin glass model, which belongs to the complexity class NP, to a quantum system with the sign problem.

Many efforts have been made to potentially overcome the numerical sign problem in certain situations, albeit usually in the settings that rely heavily on concrete problems. Several related approaches include the particle resampling in kinetic theory by filtering out high-frequency components,³³ the grid-based annihilation in quantum Boltzmann simulations,^{13,25} the fixed-node approximation in diffusion Monte Carlo,²² the annihilation of determinants in Fermion Monte Carlo,⁴ the resummation in an inchworm algorithm⁷ and the stationary phase approximation in the Wigner branching random walk.²⁶ In spite of their distinct appearances, the core of all the above approaches is essentially the same, that is, to fully utilize the cancelation of positive and negative weights, thereby reducing the growth of particle number as well as stochastic variance. This creed will be faithfully inherited in subsequent trials for a new approach.

Our approach, termed the Sequential-clustering Particle Annihilation via Discrepancy Estimation (SPADE), hybridizes sequential clustering of particles and independent random matching in each cluster, as depicted by the diagram:



The SPADE algorithm utilizes both number-theoretic and statistical properties of point distributions. Detailedly speaking, SPADE consists of two steps. The first step is to perform adaptive clustering of positive and negative particles through a sequential binary partition of the domain Q . Each time we pick up a cluster of particles and make a further split until their star discrepancies, say, the number-theoretic

irregularities, reach a prescribed threshold, partially borrowing the pioneering idea from the non-parametric density estimation method based on discrepancy sequential partitioning.¹⁶ Then it succeeds at the second step by seeking independent random matchings in each cluster, which is essentially equivalent to sampling from a finite population without replacement, and removing paired particles. In contrast to existing approaches for PA, such as ‘fixed-node approximation’,²² SPADE requires no a priori information of the exact nodal hypersurface of underlying integrands. Instead, it will ‘learn’ the nodes based on the point distribution in an adaptive manner. In a sense, SPADE can be intuitively treated as a ‘flexible-node approximation’.

From the perspective of numerical analysis, it requires to bound the error function $\mathcal{E}(f)$ and to ensure its convergence as $N \rightarrow \infty$. The interplay between the continuous integrals and discrete (combinatorial) nature of point distributions will be extensively utilized in analysis of SPADE, and the discrepancy theory directly links both sides. First, the deterministic error bounds under arbitrary matching are given with the help of the famous Koksma-Hlawka inequality^{8,15} and a combinatorial property of the star discrepancy. The obtained bound can be separated into two parts: one comes from irregularities of point distributions (measured by the star discrepancy) and the other from the variation of test function f in the sense of Hardy and Krause, without any a priori knowledge of continuity. Since only the latter implicitly depends on the dimensionality d , the error bounds may be immune to the curse of dimensionality for some good test functions. This explains why SPADE is able to achieve a satisfactory numerical accuracy for certain problems up to $d = 1080$ and work well for slow-varying test functions without continuous derivatives. Second, non-asymptotic stochastic error bounds under random matching further sharpens the deterministic ones with the help of concentration inequalities for the sum of independent random variables^{3,5,11} and sampling from a finite population without replacement.^{2,24,29} As a comparison, the optimal assignment¹⁴ is also adopted to pair the positive and negative particles in each cluster. Numerical results show that the random matching usually outperforms the optimal assignment.

The rest is organized as follows. Notations and definitions are given in Section 2, proceeding with a statement of main results in Section 3. The sequential clustering is issued in Section 4 with a proof of deterministic bounds. The random matching is discussed in Section 5 and the bounds of error function will be sharpened thanks to concentration of random variables. It follows by numerical experiments in Section 6. The paper is concluded in Section 7 with a few remarks.

Acknowledgements. This research was supported by the National Natural Science Foundation of China (Nos. 11822102, 11421101) and High-performance Computing Platform of Peking University. SS is partially supported by Beijing Academy of Artificial Intelligence (BAAI). YX is partially supported by The Elite Program of Computational and Applied Mathematics for PhD Candidates in Peking University.

2 Notations and definitions

We use the short hand notation $Q = [\mathbf{a}, \mathbf{b}] = \prod_{j=1}^d [a_j, b_j]$ to denote a hyper-rectangle in \mathbb{R}^d , where $\mathbf{a} = (a_1, \dots, a_d)$ and $\mathbf{b} = (b_1, \dots, b_d)$ with a_j and b_j specifying the lower and upper bound of Q along dimension j . A **partition** of Q at level K is denoted by $\mathcal{P}_K = \{Q_1, \dots, Q_K\}$, where $Q = \bigcup_{k=1}^K Q_k$ and $Q_k = [\mathbf{a}_k, \mathbf{b}_k]$ are mutually disjoint rectangular bins, say, $Q_i \cap Q_j = \emptyset$ for $i \neq j$. Equivalently, it means a set of d finite sequences $\eta_i^{(0)}, \dots, \eta_i^{(m_i)}$, $i = 1, \dots, d$, with

$$a_i \leq \eta_i^{(0)} \leq \dots \leq \eta_i^{(m_i)} \leq b_i,$$

by sorting the i -th coordinates of all the lower and upper bounds of Q_k in an increasing order. The collection of all partitions is denoted by \mathcal{P} .

The **subsequences** of \mathcal{X} and \mathcal{Y} in Q_k are denoted by $\mathcal{X}_k = (\mathbf{x}_1^{(k)}, \dots, \mathbf{x}_{P_k}^{(k)})$ and $\mathcal{Y}_k = (\mathbf{y}_1^{(k)}, \dots, \mathbf{y}_{M_k}^{(k)})$, respectively. $P_k = |\mathcal{X}_k|$ and $M_k = |\mathcal{Y}_k|$ are the cardinal numbers, and we let $P_k \wedge M_k = \min\{P_k, M_k\}$.

Definition 1. For two finite sequences $(\mathbf{x}_1, \dots, \mathbf{x}_P)$ and $(\mathbf{y}_1, \dots, \mathbf{y}_M)$, $P \geq M$, a **matching** is an injective function $\sigma : \{1, \dots, M\} \rightarrow \{1, \dots, P\}$. A random matching σ satisfies

$$\Pr \{(f(X_1), \dots, f(X_t)) = (f(\mathbf{x}_{\sigma(1)}), \dots, f(\mathbf{x}_{\sigma(t)}))\} = \frac{1}{P(P-1) \dots (P-t+1)} \quad (2.1)$$

for random variables X_t , $1 \leq t \leq M$, which is equivalent to sampling M times from a finite population $\{1, \dots, P\}$ without replacement. By contrast, an optimal assignment is a matching σ to attain $\min_{\sigma} \sum_{i=1}^M \|\mathbf{x}_{\sigma(i)} - \mathbf{y}_i\|$ for a given norm.

To quantitatively measure the difference between the continuous integral and the arithmetic mean of the sequences $\{f(\mathbf{x}_1), \dots, f(\mathbf{x}_P)\}$, i.e.,

$$\left| \frac{1}{\lambda(Q)} \int_Q f(\mathbf{x}) d\mathbf{x} - \frac{1}{P} \sum_{i=1}^P f(\mathbf{x}_i) \right|, \quad (2.2)$$

we need both concepts of the variation of the function f and the star discrepancy of sequence $(\mathbf{x}_1, \dots, \mathbf{x}_P)$. Here $\lambda(Q)$ gives the Lebesgue measure of Q .

Given a partition of Q , we define an operator

$$\begin{aligned} \Delta_i f(x_1, \dots, x_{i-1}, \eta_i^{(j)}, x_{i+1}, \dots, x_d) &= f(x_1, \dots, x_{i-1}, \eta_i^{(j+1)}, x_{i+1}, \dots, x_d) \\ &\quad - f(x_1, \dots, x_{i-1}, \eta_i^{(j)}, x_{i+1}, \dots, x_d). \end{aligned} \quad (2.3)$$

The **variation** of f on $[\mathbf{a}, \mathbf{b}]$ in the sense of Hardy and Krause, denoted by $V_{[\mathbf{a}, \mathbf{b}]}^{HK}(f)$,^{8,20} is delineated as follows.

Definition 2. The variation of function f on $[\mathbf{a}, \mathbf{b}]$ in the sense of Vitali reads

$$V^{(l)}(f) = \sup_{\mathcal{P}} \sum_{j_1=0}^{m_1-1} \dots \sum_{j_d=0}^{m_d-1} \left| \Delta_1 \dots \Delta_l f(\eta_1^{(j_1)}, \dots, \eta_d^{(j_d)}) \right|, \quad (2.4)$$

where the supremum is extended over all possible partitions \mathcal{P} . Then the variation of f on $[\mathbf{a}, \mathbf{b}]$ in the sense of Hardy and Krause is

$$V_{[\mathbf{a}, \mathbf{b}]}^{HK}(f) = \sum_{l=1}^d \sum_{F_l} V^{(l)}(f^{(F_l)}), \quad (2.5)$$

where $f^{(F_l)}$ presents the restriction of f to the l -dimensional face F_l of dimensions $\{i_1, i_2, \dots, i_l\} \subset \{1, \dots, d\}$, defined by $x_i = b_i$ for $i \notin \{i_1, \dots, i_l\}$, and the second sum is extended over all l -dimensional faces F_l . In particular, for continuous functions f with continuous mixed partial derivatives, we have

$$V_{[\mathbf{a}, \mathbf{b}]}^{HK}(f) = \sum_{l=1}^d \sum_{F_l} \int_{F_l} \left| \frac{\partial^l f^{(F_l)}}{\partial x_{i_1} \dots \partial x_{i_l}} \right| dx_{i_1} \dots dx_{i_l}. \quad (2.6)$$

For functions with vanishing mixed derivatives, e.g., $f(\mathbf{x}) = x_1 + \dots + x_d$ or $f(\mathbf{x}) = x_1^2 + \dots + x_d^2$, $V_{[\mathbf{a}, \mathbf{b}]}^{HK}(f)$ may depend on d linearly (see Eqs. (6.7) and (6.8)). By contrast, for $f(\mathbf{x}) = x_1 x_2 \dots x_d$, $V_{[\mathbf{a}, \mathbf{b}]}^{HK}(f)$ depends on d exponentially (see Eq. (6.11)). For the indicating function $f(\mathbf{x}) = \chi_I(\mathbf{x})$, it has that $V_{[\mathbf{a}, \mathbf{b}]}^{HK}(f) = 2^d$ for $I = [\tilde{\mathbf{a}}, \tilde{\mathbf{b}}] \subset [\mathbf{a}, \mathbf{b}]$ with $a_i < \tilde{a}_i < \tilde{b}_i < b_i$, $1 \leq i \leq d$.²⁰

Another characterization of local variation of f on $[\mathbf{a}, \mathbf{b}]$ is the **oscillator norm**:

$$\text{osc}_{[\mathbf{a}, \mathbf{b}]}(f) = \sup_{(\mathbf{x}, \mathbf{x}') \in [\mathbf{a}, \mathbf{b}]^2} |f(\mathbf{x}) - f(\mathbf{x}')|, \quad (2.7)$$

and the **local L^2 -norm** of f on \mathbf{Q} is defined by

$$\|f\|_{L^2(\mathbf{Q})} = \left(\frac{1}{\lambda(\mathbf{Q})} \int_{\mathbf{Q}} f^2(\mathbf{x}) d\mathbf{x} \right)^{1/2}. \quad (2.8)$$

The **star discrepancy**,^{8,15} stemming from number theory, is adopted to measure the irregularity of a sequence $(\mathbf{x}_1, \dots, \mathbf{x}_P) \subset [0, 1]^d$.

Definition 3. Let $\mathcal{X} = (\mathbf{x}_1, \dots, \mathbf{x}_P)$ be a finite sequence of points in the d -dimensional space $[0, 1]^d$. Then the number

$$D_P^*(\mathbf{x}_1, \dots, \mathbf{x}_P) = \sup_{\mathbf{u} \in [0, 1]^d} \left| \frac{A([\mathbf{0}, \mathbf{u}], P, \mathcal{X})}{P} - \lambda([\mathbf{0}, \mathbf{u}]) \right|, \quad (2.9)$$

is called the star discrepancy of sequence \mathcal{X} . Here $A(I, P, \mathcal{X}) = \sum_{i=1}^P \chi_I(\mathbf{x}_i)$ gives the number of the sequence \mathcal{X} in I .

For a general sequence $(\mathbf{x}_1, \dots, \mathbf{x}_P) \subset [\mathbf{a}_k, \mathbf{b}_k]$, its irregularity can be measured by the star discrepancy after mapping it from $[\mathbf{a}_k, \mathbf{b}_k]$ to $[0, 1]^d$ via a linear **scaling**:

$$\phi_k(\mathbf{x}) = \left(\frac{x_1 - a_{k,1}}{b_{k,1} - a_{k,1}}, \frac{x_2 - a_{k,2}}{b_{k,2} - a_{k,2}}, \dots, \frac{x_d - a_{k,d}}{b_{k,d} - a_{k,d}} \right). \quad (2.10)$$

In this work, we always deal with test functions in the class with bounded variations in the sense of Hardy and Krause, say, $V_{[\mathbf{a}, \mathbf{b}]}^{HK}(f) < \infty$. Under the partition \mathcal{P}_K , their oscillator norms $\text{osc}_{[\mathbf{a}_k, \mathbf{b}_k]}(f)$ are also bounded for $k = 1, \dots, K$.

3 Statement of main theorems

The SPADE algorithm consists of two steps: Clustering and matching.

Clustering: Establish a partition \mathcal{P}_K of \mathcal{Q} of level K associated with clustering of particles \mathcal{X} and \mathcal{Y} such that the star discrepancies of both clustered subsequences \mathcal{X}_k and \mathcal{Y}_k in \mathcal{Q}_k are all bounded for $k = 1, \dots, K$:

$$\begin{aligned} D_{P_k}^*(\phi_k(\mathbf{x}_1^{(k)}), \dots, \phi_k(\mathbf{x}_{P_k}^{(k)})) &\leq \frac{\vartheta\sqrt{N}}{P_k}, \\ D_{M_k}^*(\phi_k(\mathbf{y}_1^{(k)}), \dots, \phi_k(\mathbf{y}_{M_k}^{(k)})) &\leq \frac{\vartheta\sqrt{N}}{M_k}, \end{aligned} \quad (3.1)$$

where $\vartheta \in (0, 1)$ is a prescribed parameter to control the error function $\mathcal{E}(f)$.

Matching: Within each cluster, seek a matching σ from $\{1, \dots, M_k\}$ to $\{1, \dots, P_k\}$ independently when $M_k \leq P_k$, or from $\{1, \dots, P_k\}$ to $\{1, \dots, M_k\}$ when $M_k > P_k$, and then remove the matched pairs from \mathcal{X}_k and \mathcal{Y}_k .

Under the partition \mathcal{P}_K , the error function between two empirical signed measures μ (before annihilation) and ν (after annihilation) is

$$\mathcal{E}(f) = \sum_{k=1}^K \mathcal{E}_k(f), \quad (3.2)$$

$$\mathcal{E}_k(f) = \xi_k + \frac{P_k \wedge M_k}{NP_k} \sum_{i=1}^{P_k} f(\mathbf{x}_i) - \frac{P_k \wedge M_k}{NM_k} \sum_{i=1}^{M_k} f(\mathbf{y}_i), \quad (3.3)$$

$$\xi_k = \begin{cases} \frac{P_k \wedge M_k}{N} \left(\frac{1}{M_k} \sum_{i=1}^{M_k} f(\mathbf{x}_{\sigma(i)}) - \frac{1}{P_k} \sum_{i=1}^{P_k} f(\mathbf{x}_i) \right), & P_k \geq M_k, \\ \frac{P_k \wedge M_k}{N} \left(\frac{1}{M_k} \sum_{i=1}^{M_k} f(\mathbf{y}_i) - \frac{1}{P_k} \sum_{i=1}^{P_k} f(\mathbf{y}_{\sigma(i)}) \right), & P_k < M_k. \end{cases} \quad (3.4)$$

The condition (3.1) is used to bound the second and third terms in Eq. (3.3) owing to the Koksma-Hlawka inequality. As for the first term, the bound can be obtained by either the combinatorial property of the star discrepancy or the bounded difference condition $\text{osc}_{[a_k, b_k]}(f) < \infty$. It deserves to mention that K , the partition level, depends on d implicitly as the star discrepancy does. In general, K has to be smaller than total particle number N_{tot} to avoid the ‘overfitting’ phenomenon.

Theorem 1 (Deterministic bounds under arbitrary matching). *For two sequences \mathcal{X} and \mathcal{Y} under partition \mathcal{P}_K , suppose (i) there exists a constant $0 < \vartheta \leq 1$ such that the bounds of star discrepancies (3.1) hold for each cluster; (ii) there exists another constant $\gamma \in [\vartheta, 1]$ such that $P_k \wedge M_k \leq \gamma\sqrt{N}$ for each cluster. Then under arbitrary matching between \mathcal{X}_k and \mathcal{Y}_k , for any function f with bounded variation $V_{[a, b]}^{HK}(f) < \infty$ in the sense of Hardy and Krause, it has that*

$$|\mathcal{E}(f)| \leq \frac{H_0(\vartheta, \gamma)}{N^{1/2}} V_{[a, b]}^{HK}(f), \quad (3.5)$$

and

$$|\mathcal{E}(f)| \leq \frac{\gamma}{4N^{1/2}} \sum_{k=1}^K \text{osc}_{[\mathbf{a}_k, \mathbf{b}_k]}(f) + \frac{2\vartheta}{N^{1/2}} V_{[\mathbf{a}, \mathbf{b}] }^{HK}(f). \quad (3.6)$$

Here $H_0(\vartheta, \gamma) = \frac{\gamma}{4} + \frac{3\vartheta}{2} + \frac{\vartheta^2}{4\gamma}$.

The first bound (3.5), obtained using the Koksma-Hlawka inequality and the combinatorial property of star discrepancies, characterizes the basic convergence of SPADE. A key observation follows that the sole factor that may implicitly depend on dimensionality d is the variation function $V_{[\mathbf{a}, \mathbf{b}] }^{HK}(f)$. In other words, the bound (3.5) might not be bothered by the curse of dimensionality for slow-varying test functions.

The worse-case bound of $\sum_{k=1}^K \xi_k$ appears in the second bound (3.6), which turns out to be a gross over-estimate in general. A useful improvement is to adopt independent random matchings in each cluster, so that ξ_1, \dots, ξ_K become independent random variables with $\mathbb{E}\xi_k = 0$ and the sum $\sum_{k=1}^K \xi_k$ will be concentrated near the mean value zero. Meanwhile, the second and third terms in Eq. (3.3) remain non-stochastic and are bounded by the Koksma-Hlawka inequality. In consequence, stochastic upper bounds can be obtained owing to the concentration bounds of Hoeffding's type and Bernstein's type for sampling with or without replacement.^{2,5} The stochastic bounds can dramatically sharpen the deterministic worse-case bound with a high probability, albeit not tight. Furthermore, estimation of the stochastic variance $\text{Var}(\mathcal{E}(f)) = \mathbb{E}(\mathcal{E}(f) - \mathbb{E}\mathcal{E}(f))^2$ is also of the great importance for the random matching. That is equivalent to estimate

$$\text{Var}(\mathcal{E}(f)) = \sum_{k=1}^K \mathbb{E}(\mathcal{E}_k(f) - \mathbb{E}\mathcal{E}_k(f))^2 = \sum_{k=1}^K \mathbb{E}(\xi_k - \mathbb{E}\xi_k)^2 = \sum_{k=1}^K \mathbb{E}\xi_k^2. \quad (3.7)$$

Theorem 2 (Stochastic bounds under random matching). *Under the assumptions in Theorem 1 and independent random matching between \mathcal{X}_k and \mathcal{Y}_k in each cluster, for any function f with bounded variation $V_{[\mathbf{a}, \mathbf{b}] }^{HK}(f) < \infty$ in the sense of Hardy and Krause, it holds that*

$$|\mathbb{E}\mathcal{E}(f)| \leq \frac{2\vartheta}{N^{1/2}} V_{[\mathbf{a}, \mathbf{b}] }^{HK}(f), \quad (3.8)$$

and

$$\text{Var}(\mathcal{E}(f)) \leq \frac{H_1(N, \gamma)}{N^{3/2}} \sum_{k=1}^K \left(\text{osc}_{[\mathbf{a}_k, \mathbf{b}_k]}(f) \right)^2, \quad (3.9)$$

where $H_1(N, \gamma) = \frac{\gamma}{4} + \frac{1}{2N^{1/2}} + \frac{1}{4\gamma N}$. Furthermore, for any $\varepsilon \in (0, 1)$, with probability higher than $1 - \varepsilon$, it has that

$$|\mathcal{E}(f)| \leq \sqrt{2 \log(2/\varepsilon) \text{Var}(\mathcal{E}(f))} + \frac{\gamma \log(2/\varepsilon)}{6N^{1/2}} \max_k \text{osc}_{[\mathbf{a}_k, \mathbf{b}_k]}(f) + \frac{2\vartheta}{N^{1/2}} V_{[\mathbf{a}, \mathbf{b}] }^{HK}(f). \quad (3.10)$$

Eqs. (3.8) and (3.9) characterize the bounds for the bias and variance of random matching, respectively. In the sense of expectation, the bias of PA is totally

determined by the irregularity of point distributions as $\mathbb{E}\xi_k$ vanishes under sampling without replacement. It notes that the constant factor is tighter compared to Eq. (3.5) as $\gamma/4 + \vartheta^2/4\gamma \geq \vartheta/2$. The variance of random matching is of the order $N^{-3/2}$ and the constant factor relies on the oscillator norm of f .

The bound (3.10) may dramatically improve (3.6). For the first term, the constant factor is sharpened as $\sum_{k=1}^K (\text{osc}_{[\mathbf{a}_k, \mathbf{b}_k]}(f))^2 \leq \left(\sum_{k=1}^K \text{osc}_{[\mathbf{a}_k, \mathbf{b}_k]}(f)\right)^2$ and $\text{osc}_{[\mathbf{a}_k, \mathbf{b}_k]}(f) \geq 0$. Actually, it gains an extra rate of $N^{-1/4}$. For the second term, the constant factor is diminished provided

$$\log(2/\varepsilon) \max_k \text{osc}_{[\mathbf{a}_k, \mathbf{b}_k]}(f) \leq \frac{3}{2} \sum_{k=1}^K \text{osc}_{[\mathbf{a}_k, \mathbf{b}_k]}(f).$$

The third term keeps unchanged due to the bias of matching. Therefore, with a high probability, the random matching is advantageous due to the concentration property near the mean value $\sum_{k=1}^K \mathbb{E}\xi_k = 0$.

We shall provide an alternative estimation of $\text{Var}(\mathcal{E}(f))$ by taking the irregularity of point distribution into account under an additional assumption that f^2 has a bounded variation. The discrepancy theory will be again used for bounding the local variance of random matching in each cluster, which in turn give an estimate of the second moment $\sum_{k=1}^K \mathbb{E}\xi_k^2$.

Theorem 3 (Variance estimation via bounding discrepancies). *Under the assumptions in Theorem 1 and Theorem 2, for any function f with bounded variations $V_{[\mathbf{a}, \mathbf{b}]}^{HK}(f) < \infty$ and $V_{[\mathbf{a}, \mathbf{b}]}^{HK}(f^2) < \infty$ in the sense of Hardy and Krause, it holds that*

$$\begin{aligned} \text{Var}(\mathcal{E}(f)) &\leq \frac{\vartheta H_2(N)}{N^{1/2}(N+1)} \left(V_{[\mathbf{a}, \mathbf{b}]}^{HK}(f^2) + V_{[\mathbf{a}, \mathbf{b}]}^{HK}(f) \cdot \sup_{[\mathbf{a}, \mathbf{b}]} |f| \right) \\ &\quad + \frac{\gamma H_2(N)}{N^{1/2}(N+1)} \sum_{k=1}^K \|f\|_{L^2([\mathbf{a}_k, \mathbf{b}_k])} \cdot \text{osc}_{[\mathbf{a}_k, \mathbf{b}_k]}(f) + \frac{H_3(\gamma, N)}{N(N+1)} \sum_{k=1}^K \left(\text{osc}_{[\mathbf{a}_k, \mathbf{b}_k]}(f) \right)^2, \end{aligned} \quad (3.11)$$

where $H_2(N) = \frac{9 \log(2(N+1))}{2}$ and $H_3(\gamma, N) = \frac{2(8+3\sqrt{2})^2 \log^2(2(N+1))}{9} + \frac{\gamma^2}{16}$.

By a comparison between the bounds (3.9) and (3.11), it is seen that the constant factor in the leading term of order $N^{-3/2}$ is replaced by a term composed of $\vartheta V_{[\mathbf{a}, \mathbf{b}]}^{HK}(f^2)$, $\vartheta V_{[\mathbf{a}, \mathbf{b}]}^{HK}(f) \cdot \sup_{[\mathbf{a}, \mathbf{b}]} |f|$ and $\sum_{k=1}^K \|f\|_{L^2([\mathbf{a}_k, \mathbf{b}_k])} \cdot \text{osc}_{[\mathbf{a}_k, \mathbf{b}_k]}(f)$, which may be tighter than $\sum_{k=1}^K (\text{osc}_{[\mathbf{a}_k, \mathbf{b}_k]}(f))^2$ when ϑ is sufficiently small and $|f| < 1$. The last term in Eq. (3.11) may be neglected due to the extra order of $N^{-1/2}$. Inserting Eq. (3.11) into Eq. (3.10) yields another concentration bound for random matching.

4 Clustering and discrepancy theory

As the first and crucial step of the SPADE algorithm, the clustering of particles is to divide the PA problem into several local parts. The prototype is the grid-based annihilation,^{1, 13, 25} in which the domain is partitioned into bins of equal size,

so that the positive and negative particles located in the same bin are annihilated. Apparently, the advantage of such method is its simplicity and the numerical errors are controlled by the bin size.³¹ It is also closely related to the histogram statistics in non-parametric density estimation since the annihilation can be realized based on the difference of two probability densities postulated from positive and negative particles, respectively.

However, the setting of uniform grid is no longer applicable for higher dimensional PA problem arising in particle simulations of many-body problems. The reasons are as twofold. First, the number of bins grows exponentially in d , known as the curse of dimensionality. Second, the required sample size for given accuracy also grows with the increasing number of bins.³¹ A potential way to resolve these challenges is to replace the uniform grid mesh by an adaptive one driven by the distribution of particle populations, borrowing the basic idea from high-dimensional statistical learning theory.^{16,17} However, the negative weights emerged in the PA problem make it essentially different from the density estimation.

In practice, an adaptive partition is established through the sequential binary splitting, which in turn clusters positive and negative particles in a hierarchical manner. Two key ingredients must be specified for the adaptive partition. One is the criterion for stopping the binary splitting. SPADE tries to utilize the number-theoretical properties (discrepancy) of two kinds of particles to make the decision like in discrepancy sequential partitioning,¹⁶ instead of relying on any a priori probability distribution as adopted in the Bayesian interference.¹⁷ The other is the choice of nodes to be split, which is relevant in monitoring the nodal hyper-surfaces of underlying integrand function. SPADE chooses a node to maximize a gap function between the distributions of positive and negative particles.

4.1 Setting of sequential clustering

An adaptive partition is built up through the binary splitting. The binary partition can be defined in the following recursively way. It starts with $\mathcal{P}_0 = \mathcal{Q}$. Suppose at level K we have $\mathcal{P}_K = \{\mathcal{Q}_1, \mathcal{Q}_2, \dots, \mathcal{Q}_K\}$ with \mathcal{Q}_k mutually disjoint and $\mathcal{Q} = \cup_{k=1}^K \mathcal{Q}_k$, then the binary partition at level $K + 1$ is obtained by choosing one sub-rectangle \mathcal{Q}_k and dividing it into two parts along one of its coordinate, parallel to one of dimensions.

For example, for $\mathcal{Q}_k = [\mathbf{a}_k, \mathbf{b}_k]$, we pick up j -th dimension and choose a node $c_{k,j} \in (a_{k,j}, b_{k,j})$. Then \mathcal{Q}_k is split into $\mathcal{Q}_k = \mathcal{Q}_k^{(1)} \cup \mathcal{Q}_k^{(2)}$ with

$$\begin{aligned} \mathcal{Q}_k^{(1)} &= \prod_{i=1}^{j-1} [a_{k,i}, b_{k,i}] \times [a_{k,j}, c_{k,j}] \times \prod_{i=j+1}^d [a_{k,i}, b_{k,i}], \\ \mathcal{Q}_k^{(2)} &= \prod_{i=1}^{j-1} [a_{k,i}, b_{k,i}] \times [c_{k,j}, b_{k,j}] \times \prod_{i=j+1}^d [a_{k,i}, b_{k,i}]. \end{aligned} \tag{4.1}$$

We can establish the partition \mathcal{P}_{K+1} at level $K + 1$ by

$$\mathcal{P}_{K+1} = (\mathcal{P}_K \setminus \mathcal{Q}_k) \cup \mathcal{Q}_k^{(1)} \cup \mathcal{Q}_k^{(2)}, \tag{4.2}$$

Algorithm 1 Clustering via adaptive partitioning

```

function ( $\{\mathcal{X}_1, \dots, \mathcal{X}_K\}, \{\mathcal{Y}_1, \dots, \mathcal{Y}_K\}$ ) = CLUSTERING( $\mathcal{X}, \mathcal{Y}, \mathcal{Q}, \vartheta$ )
   $K = 1, \mathcal{Q}_1 = \mathcal{Q}, \mathcal{X}_1 = \mathcal{X}, \mathcal{Y}_1 = \mathcal{Y}, \mathcal{P} = \{\mathcal{Q}_1\}, \mathcal{P}' = \emptyset.$ 
  while  $\mathcal{P} \neq \mathcal{P}'$  do
     $\mathcal{P}' = \mathcal{P}$ 
    for all  $\mathcal{Q}_k = [a_k, b_k]$  in  $\mathcal{P}, k \leq K$  do
       $\mathcal{P} \leftarrow \mathcal{P} \setminus \mathcal{Q}_k, \mathcal{X} \leftarrow \mathcal{X} \setminus \mathcal{X}_k, \mathcal{Y} \leftarrow \mathcal{Y} \setminus \mathcal{Y}_k$ 
      Scale all  $\mathbf{x}_i \in \mathcal{Q}_k$  to  $\phi_k(\mathbf{x}_i) \in [0, 1]^d$  and  $\mathbf{y}_i \in \mathcal{Q}_k$  to  $\phi_k(\mathbf{y}_i) \in [0, 1]^d$ 
      Calculate the star discrepancy  $\text{disc}_+ = D_{P_k}^*(\phi_k(\mathbf{x}_1^{(k)}), \dots, \phi_k(\mathbf{x}_{P_k}^{(k)}))$ 
      Calculate the star discrepancy  $\text{disc}_- = D_{M_k}^*(\phi_k(\mathbf{y}_1^{(k)}), \dots, \phi_k(\mathbf{y}_{M_k}^{(k)}))$ 
      if  $\text{disc}_+ > \frac{\vartheta\sqrt{N}}{P_k}$  or  $\text{disc}_- > \frac{\vartheta\sqrt{N}}{M_k}$  then
         $K \leftarrow K + 1$ 
        Choose a node  $c_{k,j}$  to attain the maximum of Eq. (4.4)
        Divide the sub-region  $\mathcal{Q}_k$  into  $\mathcal{Q}_k^{(1)}$  and  $\mathcal{Q}_k^{(2)}$  as given in Eq. (4.1)
        Divide the pointsets:  $\mathcal{X}_k = \mathcal{X}_k^{(1)} \cup \mathcal{X}_k^{(2)}$  and  $\mathcal{Y}_k = \mathcal{Y}_k^{(1)} \cup \mathcal{Y}_k^{(2)}$ 
        Update the partition:  $\mathcal{P} \leftarrow \mathcal{P} \cup \mathcal{Q}_k^{(1)} \cup \mathcal{Q}_k^{(2)},$ 
        Update the particle sets:  $\mathcal{X} \leftarrow \mathcal{X} \cup \mathcal{X}_k^{(1)} \cup \mathcal{X}_k^{(2)}, \mathcal{Y} \leftarrow \mathcal{Y} \cup \mathcal{Y}_k^{(1)} \cup \mathcal{Y}_k^{(2)}$ 
      else
         $\mathcal{P} \leftarrow \mathcal{P} \cup \mathcal{Q}_k, \mathcal{X} \leftarrow \mathcal{X} \cup \mathcal{X}_k, \mathcal{Y} \leftarrow \mathcal{Y} \cup \mathcal{Y}_k$ 
      end if
    end for
  end while
  return  $\mathcal{X} = \{\mathcal{X}_1, \dots, \mathcal{X}_K\}, \mathcal{Y} = \{\mathcal{Y}_1, \dots, \mathcal{Y}_K\}, \mathcal{P}_K = \mathcal{P} = \{\mathcal{Q}_1, \dots, \mathcal{Q}_K\}$ 
end function

```

and $\mathcal{X}_k = \mathcal{X}_k^{(1)} \cup \mathcal{X}_k^{(2)}, \mathcal{Y}_k = \mathcal{Y}_k^{(2)} \cup \mathcal{Y}_k^{(1)}$ with $P_k^{(i)} = |\mathcal{X}_k^{(i)}|, M_k^{(i)} = |\mathcal{Y}_k^{(i)}|$, respectively.

Although there are various choices of $c_{k,j}$, a rule of thumb for PA is to dig out the possible nodal points in the hyper-surfaces of the underlying integrand function. To this end, we can adopt the following strategy in practice. We can pick up the j -th dimension and m equidistant points in the interval $[a_{k,j}, b_{k,j}]$:

$$c_{k,j} = a_{k,j} + \frac{l}{m}(b_{k,j} - a_{k,j}), \quad l = 1, \dots, m - 1, \quad (4.3)$$

then select the node $c_{k,j}$ from $(m - 1) \times d$ choices (typically, $m = 2, 4, 8$) to attain the maximal value of the following **difference gap**:

$$\left| \frac{P_k^{(1)}}{P_k} - \frac{M_k^{(1)}}{M_k} \right| + \left| \frac{P_k^{(2)}}{P_k} - \frac{M_k^{(2)}}{M_k} \right| = 2 \left| \frac{P_k^{(1)}}{P_k} - \frac{M_k^{(1)}}{M_k} \right|, \quad (4.4)$$

which measures the gap between the distributions of positive and negative particles after splitting. Heuristically, a large difference gap means positive and negative particles tend to concentrate in different bins. That is, concentrations of positive or negative particles should be observed in opposite sides of the nodal hyper-surfaces.

4.2 Deterministic bounds under arbitrary matching

The clustering allows us to analyze the error function $\mathcal{E}(f)$ by bounding the local pieces $\mathcal{E}_k(f)$, which depend on both variations of test function f and the bounds for star discrepancies of \mathcal{X}_k and \mathcal{Y}_k due to the celebrated Koksma-Hlawka inequality.

In fact, the discrepancy theory plays a crucial role in high-dimensional numerical analysis and the most outstanding application is the low-discrepancy sequence in numerical integration, known as the quasi-Monte Carlo method.^{6,19} Owing to the deterministic sequences with the star discrepancy of the order $(\log n)^d/n$, where n is the required number of samples, the quasi-Monte Carlo achieves a theoretical convergence order of n^{-1} , but may still lose its effectiveness in higher dimension due to the factor $(\log n)^d$.^{6,28} Nonetheless, in certain applications it has been reported to obtain a satisfactory accuracy in evaluating the integrations up to $d = 360$.²¹

Here we would like to focus on the potential application of discrepancy theory in clustering, without any specified construction of low-discrepancy sequences. It deserves to mention that the bounds of star discrepancies given in Eq. (3.1) are still of order n^{-1} with n the count of sequences, but their numerators are free from dimensionality d . As a consequence, in the deterministic bounds for SPADE as stated in Theorem 1, the dependence on d is only embodied in the variation of test function, instead of the irregularity of points.

We begin to prove Theorem 1. Before that, we need Lemma 1 on the summation property and scaling-invariant property of variation in the sense of Hardy and Krause,²⁰ as well as Lemma 2 on the combinatorial property of the star discrepancy.

Lemma 1. *Let f be defined on the hyper-rectangle $Q = [\mathbf{a}, \mathbf{b}]$, $\{Q_1, \dots, Q_K\}$, $Q_k = [\mathbf{a}_k, \mathbf{b}_k]$, $k = 1, \dots, K$ be a binary partition of Q . Then*

$$V_{[\mathbf{a}, \mathbf{b}]}^{HK}(f) = \sum_{k=1}^K V_{[\mathbf{a}_k, \mathbf{b}_k]}^{HK}(f). \quad (4.5)$$

In addition, suppose ϕ is strictly monotone increasing function from $[\mathbf{a}, \mathbf{b}]$ onto $[0, 1]^d$, say, for $x_i^{(1)} < x_i^{(2)}$, $1 \leq i \leq d$,

$$\phi(x_1, \dots, x_{i-1}, x_i^{(1)}, x_i, \dots, x_d) < \phi(x_1, \dots, x_{i-1}, x_i^{(2)}, x_i, \dots, x_d).$$

Let $\tilde{f}(\tilde{\mathbf{x}}) = f(\mathbf{x})$ with $\tilde{\mathbf{x}} = \phi(\mathbf{x})$, then $V_{[\mathbf{a}, \mathbf{b}]}^{HK}(f) = V_{[0, 1]^d}^{HK}(\tilde{f})$.

The proof of Lemma 1 can be found in.²⁰ Combining the Koksma-Hlawka inequality and Lemma 1 yields the generalized Koksma-Hlawka inequality.

Proposition 1 (Generalized Koksma-Hlawka inequality). *Let f be of bounded variation on $Q = [\mathbf{a}, \mathbf{b}]$ in the sense of Hardy and Krause and ϕ is linear scaling from $Q = [\mathbf{a}, \mathbf{b}]$ to $[0, 1]^d$. Then for any sequence $\mathcal{X} = (\mathbf{x}_1, \dots, \mathbf{x}_P) \subset Q^P$, it has that*

$$\left| \frac{1}{P} \sum_{i=1}^P f(\mathbf{x}_i) - \frac{1}{\lambda(Q)} \int_Q f(\mathbf{x}) d\mathbf{x} \right| \leq V_{[\mathbf{a}, \mathbf{b}]}^{HK}(f) \cdot D_P^*(\phi(\mathbf{x}_1), \dots, \phi(\mathbf{x}_P)). \quad (4.6)$$

Proof. Since the scaling ϕ is strictly monotone increasing, we have that

$$\begin{aligned} \left| \frac{1}{P} \sum_{i=1}^P f(\mathbf{x}_i) - \frac{1}{\lambda(Q)} \int_Q f(\mathbf{x}) d\mathbf{x} \right| &= \left| \frac{1}{P} \sum_{i=1}^P \tilde{f}(\phi(\mathbf{x}_i)) - \int_{[0,1]^d} \tilde{f}(\tilde{\mathbf{x}}) d\tilde{\mathbf{x}} \right| \\ &\leq V_{[0,1]^d}^{HK}(\tilde{f}) \cdot D_P^*(\phi(\mathbf{x}_1), \dots, \phi(\mathbf{x}_P)) \\ &= V_{[a,b]}^{HK}(f) \cdot D_P^*(\phi(\mathbf{x}_1), \dots, \phi(\mathbf{x}_P)), \end{aligned}$$

where the second inequality is the standard Koksma-Hlawka inequality, and the last one uses Lemma 1. \square

In order to characterize the star discrepancy of a subsequence after removing k points, we need a combinatorial lemma.

Lemma 2 (Combinatorial property of star discrepancy). *For any sequence $\mathcal{X} = (\mathbf{x}_1, \dots, \mathbf{x}_P) \subset [0, 1]^{d \times P}$ and arbitrary k points $\mathcal{X}_k \subset \mathcal{X}$ in it, we have that*

$$D_{P-k}^*(\{\mathbf{x}_1, \dots, \mathbf{x}_P\} \setminus \mathcal{X}_k) \leq D_P^*(\mathbf{x}_1, \dots, \mathbf{x}_P) + \frac{k}{P}. \quad (4.7)$$

Proof. Suppose I is the critical box¹⁸ that attains the star discrepancy of the sequence $\{\mathbf{x}_1, \dots, \mathbf{x}_P\} \setminus \mathcal{X}_k$, then

$$\begin{aligned} &D_{P-k}^*(\{\mathbf{x}_1, \dots, \mathbf{x}_P\} \setminus \mathcal{X}_k) - D_P^*(\mathbf{x}_1, \dots, \mathbf{x}_P) \\ &\leq \left| \frac{A(I, P-k, \mathcal{X} \setminus \mathcal{X}_k)}{P-k} - \lambda(I) \right| - \left| \frac{A(I, P, \mathcal{X})}{P} - \lambda(I) \right| \\ &\leq \left| \frac{A(I, P-k, \mathcal{X} \setminus \mathcal{X}_k)}{P-k} - \frac{A(I, P, \mathcal{X})}{P} \right|. \end{aligned}$$

Since $0 \leq A(I, P, \mathcal{X}) - A(I, P-k, \mathcal{X} \setminus \mathcal{X}_k) \leq k$, it suffices to take $A(I, P, \mathcal{X}) - A(I, P-k, \mathcal{X} \setminus \mathcal{X}_k) = m$. Then

$$\left| \frac{A(I, P-k, \mathcal{X} \setminus \mathcal{X}_k)}{P-k} - \frac{A(I, P, \mathcal{X})}{P} \right| = \left| \frac{kA(I, P-k, \mathcal{X} \setminus \mathcal{X}_k)}{P(P-k)} - \frac{m}{P} \right| \leq \frac{k}{P}.$$

The last inequality utilizes the fact that

$$0 \leq \frac{kA(I, P-k, \mathcal{X} \setminus \mathcal{X}_k)}{P(P-k)} \leq \frac{k}{P}$$

and $m \leq k$. The proof is completed. \square

Now we give a deterministic bound for ξ_k in Eq. (3.3), which also bounds the random variables in Section 5.

Lemma 3 (A deterministic bound for random variables). *Suppose $P_k \wedge M_k \leq \gamma\sqrt{N}$ and $\text{osc}_{[a_k, b_k]}(f) < \infty$, then it has that*

$$|\xi_k| \leq \frac{\gamma}{4\sqrt{N}} \text{osc}_{[a_k, b_k]}(f). \quad (4.8)$$

Proof. It suffices to consider $P_k \geq M_k$. From Eq. (3.4), a direct calculation yields

$$\begin{aligned} |\xi_k| &= \frac{1}{NP_k} \left| P_k \sum_{i=1}^{M_k} f(\mathbf{x}_{\sigma(i)}) - M_k \sum_{i=1}^{P_k} f(\mathbf{x}_i) \right| \\ &= \frac{1}{NP_k} \left| (P_k - M_k) \sum_{i=1}^{M_k} f(\mathbf{x}_{\sigma(i)}) - M_k \sum_{i=1}^{P_k} f(\mathbf{x}_i) + M_k \sum_{i=1}^{M_k} f(\mathbf{x}_{\sigma(i)}) \right|. \end{aligned}$$

Since

$$(P_k - M_k) \sum_{i=1}^{M_k} f(\mathbf{x}_{\sigma(i)}) = \sum_{i=1}^{M_k} \sum_{j=1}^{P_k - M_k} f(\mathbf{x}_{\sigma(i)}^{(j)})$$

with $\mathbf{x}_{\sigma(i)}^{(j)}$ being the copy of $\mathbf{x}_{\sigma(i)}$, it has that

$$|\xi_k| \leq \frac{(P_k - M_k)M_k}{NP_k} \operatorname{osc}_{[\mathbf{a}_k, \mathbf{b}_k]}(f) \leq \frac{P_k}{4N} \operatorname{osc}_{[\mathbf{a}_k, \mathbf{b}_k]}(f) \leq \frac{\gamma}{4\sqrt{N}} \operatorname{osc}_{[\mathbf{a}_k, \mathbf{b}_k]}(f).$$

□

With these preparations, we are able to finish the proof of Theorem 1.

Proof of Theorem 1. Suppose $P_k \geq M_k$ for the k -th cluster. Let \mathcal{X}_k^A and \mathcal{Y}_k^A denote the particles after removal, $|\mathcal{X}_k^A| = P_k - P_k \wedge M_k$ and $|\mathcal{Y}_k^A| = M_k - P_k \wedge M_k$. According to Proposition 1, it has that

$$\begin{aligned} |\mathcal{E}_k(f)| &= \frac{M_k}{N} \left| \frac{1}{M_k} \sum_{\mathcal{X}_k \setminus \mathcal{X}_k^A} f(\mathbf{x}_i) - \frac{1}{M_k} \sum_{\mathcal{Y}_k} f(\mathbf{y}_i) \right| \\ &\leq \frac{M_k}{N} D_{M_k}^*((\mathbf{x}_1, \dots, \mathbf{x}_{P_k}) \setminus \mathcal{X}_k^A) \cdot V_{[\mathbf{a}_k, \mathbf{b}_k]}^{HK}(f) + \frac{M_k}{N} D_{M_k}^*(\mathbf{y}_1, \dots, \mathbf{y}_{M_k}) \cdot V_{[\mathbf{a}_k, \mathbf{b}_k]}^{HK}(f). \end{aligned}$$

For the first term, when $P_k \geq \vartheta\sqrt{N}$, using Lemma 2 yields

$$\begin{aligned} \frac{M_k}{N} D_{M_k}^*((\mathbf{x}_1, \dots, \mathbf{x}_{P_k}) \setminus \mathcal{X}_k^A) &\leq \frac{M_k}{N} \frac{\vartheta\sqrt{N} + P_k - M_k}{P_k} \leq \frac{(\vartheta\sqrt{N} + P_k)^2}{4P_k N} \\ &= \frac{P_k}{4N} + \frac{\vartheta^2}{4P_k} + \frac{\vartheta}{2\sqrt{N}} \leq \frac{1}{\sqrt{N}} \left(\frac{\gamma}{4} + \frac{\vartheta}{2} + \frac{\vartheta^2}{4\gamma} \right), \end{aligned}$$

since the maximal value of $P_k/N + \vartheta^2/P_k$ for $P_k \in [\vartheta\sqrt{N}, \gamma\sqrt{N}]$ is attained at $P_k = \gamma\sqrt{N}$.

When $M_k \leq P_k < \vartheta\sqrt{N}$, the bound of discrepancy becomes trivial since

$$D_{M_k}^*((\mathbf{x}_1, \dots, \mathbf{x}_{P_k}) \setminus \mathcal{X}_k^A) \leq 1 \leq \frac{\vartheta\sqrt{N}}{P_k} \leq \frac{\vartheta\sqrt{N}}{M_k}.$$

In this case, we use the fact that

$$\frac{M_k}{N} D_{M_k}^*((\mathbf{x}_1, \dots, \mathbf{x}_{P_k}) \setminus \mathcal{X}_k^A) \leq \frac{M_k}{N} \leq \frac{\vartheta}{\sqrt{N}} \leq \frac{1}{\sqrt{N}} \left(\frac{\gamma}{4} + \frac{\vartheta}{2} + \frac{\vartheta^2}{4\gamma} \right).$$

The second term is bounded by $\frac{\vartheta}{\sqrt{N}}V_{[\mathbf{a}_k, \mathbf{b}_k]}^{HK}(f)$ due to Eq. (3.1). Summing over K terms arrives at Eq. (3.5).

As for the bound in Eq. (3.6), according to Eq. (3.3), it has that

$$\begin{aligned}
|\mathcal{E}_k(f)| &\leq |\xi_k| + \frac{M_k}{N} \left| \frac{1}{P_k} \sum_{i=1}^{P_k} f(\mathbf{x}_i) - \frac{1}{\lambda(Q_k)} \int_{Q_k} f(\mathbf{x}) d\mathbf{x} \right| \\
&\quad + \frac{M_k}{N} \left| \frac{1}{M_k} \sum_{i=1}^{M_k} f(\mathbf{y}_i) - \frac{1}{\lambda(Q_k)} \int_{Q_k} f(\mathbf{x}) d\mathbf{x} \right| \\
&\leq \frac{\gamma}{4\sqrt{N}} \text{osc}_{[\mathbf{a}_k, \mathbf{b}_k]}(f) + \frac{M_k}{N} D_{P_k}^*(\phi_k(\mathbf{x}_1), \dots, \phi_k(\mathbf{x}_{P_k})) \cdot V_{[\mathbf{a}_k, \mathbf{b}_k]}^{HK}(f) \\
&\quad + \frac{M_k}{N} D_{M_k}^*(\phi_k(\mathbf{y}_1), \dots, \phi_k(\mathbf{y}_{M_k})) \cdot V_{[\mathbf{a}_k, \mathbf{b}_k]}^{HK}(f) \\
&\leq \frac{\gamma}{4\sqrt{N}} \text{osc}_{[\mathbf{a}_k, \mathbf{b}_k]}(f) + \frac{2\vartheta}{\sqrt{N}} V_{[\mathbf{a}_k, \mathbf{b}_k]}^{HK}(f),
\end{aligned} \tag{4.9}$$

where the second inequality uses Proposition 1 and Lemma 3. \square

A remarkable observation in the proof of Theorem 1 is that the worse-case upper bound of error function is attained when $M_k = (P_k + \vartheta\sqrt{N})/2$. Actually it accords with our intuition. If M_k is sufficiently small, only a few particles are removed and errors should be small. When M_k approaches to P_k , the bound of discrepancy for \mathcal{Y}_k also controls the errors. A bad situation may occur when M_k is close to $P_k/2$.

5 Matching and concentration inequalities

The matching of two kinds of particles is the second issue we would like to address. Intuitively, we can pair the particles that are ‘sufficiently close to each other’ and resort to combinatorial algorithms for solving optimal assignment problems.¹⁴ However, the choice of metrics is rather subtle since the Euclidian distance is highly influenced by dimensionality d and an embarrassing power factor $1/d$ seems to inevitably occur in error bounds (for instance, see²⁷). Besides, we would like to extend our discussion to a general class of functions, such as that of bounded variation, and drop the assumption of continuity. For these purposes, it requires us to fully utilize the discrete nature of point distributions.

In this section, we would like to show that the random matching, in spite of its simple setting, proves to be surprisingly efficient and accurate. When $P_k \geq M_k$, a random matching from \mathcal{Y}_k to \mathcal{X}_k is equivalent to sampling M_k times from a finite population \mathcal{X}_k without replacement, and several powerful concentration inequalities will characterize the non-asymptotic bounds for the random variables ξ_k in Eq. (3.3) and their independent sum $\sum_{k=1}^K \xi_k$.

Roughly speaking, the concentration inequalities used in our analysis are divided into two categories. One is for sampling with replacement, initialized by the pioneering works of Hoeffding, Bennett and Bernstein,^{3,11} which characterizes the concentration behaviors of $\sum_{k=1}^K \xi_k$. The other category is for sampling without

replacement, realized first by Serfling,²⁴ which bounds the random variables ξ_k with a martingale structure. The latter has later been improved by Bardenet and Maillard.² The Talagrand-type inequality of sampling without replacement was given by Tolstikhin.²⁹

There are still a vast of researches on concentration inequalities and a good survey can be found in.⁵ An exhaustion of them is definitely beyond the scope of this article. Here we only use several typical concentration inequalities, such as those of Hoeffding's type and Bernstein's type. The first part mainly discusses Bernstein's inequality and the Serfling-Hoeffding inequality. The second part concentrates on the Serfling-Bernstein inequality. Again, the discrepancy theory will be used for bounding the local variance in sampling without replacement.

5.1 Stochastic bounds under random matching

We first investigate the Serfling-Hoeffding concentration inequalities for sampling without replacement. Without loss of generality, we consider the situation that the number of positive particles is no less than that of negative particles.

Consider the partial summation

$$S_k = \sum_{t=1}^k f(X_t), \quad (5.1)$$

where X_t are randomly sampled from a finite population $\mathcal{X} = (\mathbf{x}_1, \dots, \mathbf{x}_P)$ without replacement as defined in Eq. (2.1). It is easy to verify that

$$\frac{\mathbb{E}S_k}{k} - \frac{S_P}{P} = \mathbb{E} \left(\frac{1}{k} \sum_{t=1}^k f(X_t) - \frac{1}{P} \sum_{i=1}^P f(\mathbf{x}_i) \right) = 0, \quad (5.2)$$

and the two-side tail probabilities $U_M(\delta)$ and $V_M(\delta)$

$$U_M(\delta) = \Pr \left\{ \max_{M \leq k \leq P-1} \left| \frac{S_k}{k} - \frac{1}{P} \sum_{i=1}^P f(\mathbf{x}_i) \right| \geq \delta \right\}, \quad (5.3)$$

$$V_M(\delta) = \Pr \left\{ \max_{1 \leq k < M} \left| \frac{S_k}{P-k} - \frac{1}{P} \sum_{i=1}^P f(\mathbf{x}_i) \right| \geq \frac{M\delta}{P-M} \right\} \quad (5.4)$$

are bounded by the Serfling-Hoeffding inequality, which characterizes the deviation between S_k/k and the arithmetic mean of \mathcal{X} . Here we only list the concentration bounds in Lemma 4 and the detailed proof can be found in.²

Lemma 4 (The Hoeffding-Serfling inequality). *For $\mathcal{X} = (\mathbf{x}_1, \dots, \mathbf{x}_P) \subset \mathbb{Q}^P$, $\mathbb{Q} = [\mathbf{a}, \mathbf{b}]$, let (X_1, \dots, X_M) be a list of a flexible size $M < P$ sampled without replacement from \mathcal{X} . Then for any function f with bounded oscillator norm $\text{osc}_{[\mathbf{a}, \mathbf{b}]}(f) < \infty$ and $\delta > 0$, we have*

$$\begin{aligned} U_M(\delta) &\leq 2 \exp \left(\frac{-2M\delta^2}{(1 - M/P)(1 + 1/M)(\text{osc}_{[\mathbf{a}, \mathbf{b}]}(f))^2} \right), \\ V_M(\delta) &\leq 2 \exp \left(\frac{-2M\delta^2}{(1 - (M-1)/P)(\text{osc}_{[\mathbf{a}, \mathbf{b}]}(f))^2} \right). \end{aligned} \quad (5.5)$$

Moreover, for any $\varepsilon \in (0, 1)$, it holds with probability higher than $1 - \varepsilon$ that

$$\left| \frac{1}{M} \sum_{t=1}^M f(X_t) - \frac{1}{P} \sum_{i=1}^P f(\mathbf{x}_i) \right| \leq \underset{[\mathbf{a}, \mathbf{b}]}{\text{osc}}(f) \sqrt{\frac{\rho_M \log(2/\varepsilon)}{2M}}, \quad (5.6)$$

where

$$\rho_M = \begin{cases} \left(1 - \frac{M-1}{P}\right), & M < P/2, \\ \left(1 - \frac{M}{P}\right) \left(1 + \frac{1}{M}\right), & M \geq P/2. \end{cases} \quad (5.7)$$

Note in passing that Eq. (5.6) holds for $P = M$, too.

The factor M/P in Eq. (5.7) for ρ_M reflects the influence of sampling fraction²⁴ and leads to stronger concentration compared to independent sampling.²⁹

We would like to use Lemma 4 to bound the random variable

$$\xi = \frac{M}{N} \left(\frac{1}{M} \sum_{t=1}^M f(X_t) - \frac{1}{P} \sum_{i=1}^P f(\mathbf{x}_i) \right), \quad (5.8)$$

which corresponds to ξ_k in the local error term (3.3). A key observation is that $\sqrt{M\rho_M} = 0$ when $M = 0$ or $M = P$, and $\sqrt{M\rho_M}$ attains its maximal value at $M = \frac{P+1}{2}$. This coincides with our intuition since $M = 0$ means no particle is annihilated, while $M = P$ corresponds to the case in which all positive particles are selected from the population, so that errors induced by random matching vanish.

Proposition 2 (The first stochastic bound for random variables). *Suppose $P \geq M$, then any $\varepsilon \in (0, 1)$, it holds with probability higher than $1 - \varepsilon$ that*

$$|\xi| \leq \sqrt{\frac{\log(2/\varepsilon)}{8}} \left(\frac{P+1}{N\sqrt{P}} \right) \underset{[\mathbf{a}, \mathbf{b}]}{\text{osc}}(f) \quad (5.9)$$

for any function f with $\underset{[\mathbf{a}, \mathbf{b}]}{\text{osc}}(f) < \infty$. In particular, when $P \leq \gamma\sqrt{N}$, it has that

$$|\xi| \leq \sqrt{\frac{\log(2/\varepsilon)}{8}} \left(\gamma^{1/2} + \frac{1}{\gamma^{1/2}N^{1/2}} \right) \frac{\underset{[\mathbf{a}, \mathbf{b}]}{\text{osc}}(f)}{N^{3/4}}. \quad (5.10)$$

Proof. It can be readily verified from Eq. (5.7) that

$$\frac{M}{N} \sqrt{\frac{\rho_M}{M}} \leq \frac{P+1}{2N\sqrt{P}}. \quad (5.11)$$

Applying the concentration inequality (5.6) into Eq. (5.8) and using Eq. (5.11) gives Eq. (5.9).

Inserting

$$\sqrt{P} + \frac{1}{\sqrt{P}} \leq \gamma^{1/2}N^{1/4} + \frac{1}{\gamma^{1/2}N^{1/4}}, \quad 1 \leq P \leq \gamma\sqrt{N}$$

into Eq. (5.9) yields Eq. (5.10). \square

The variance estimation of the random matching is also obtained by Lemma 4. In contrast to a trivial bound obtained from Eq. (4.8):

$$\mathbb{E}\xi^2 \leq \frac{\gamma^2 (\text{osc}_{[\mathbf{a}, \mathbf{b}]}(f))^2}{16N}, \quad (5.12)$$

we would like to show that the second moment $\mathbb{E}\xi^2$ gains an extra order of $N^{-1/2}$ with the concentration bound in Eq. (5.5).

Proposition 3 (The first bound for the variance of random matching). *Suppose $P \geq M > 0$, $\text{osc}_{[\mathbf{a}, \mathbf{b}]}(f) < \infty$ and there exists a constant $\gamma < 1$ such that $P < \gamma\sqrt{N}$, then*

$$\mathbb{E}\xi^2 \leq H_1(N, \gamma) \left(\frac{\text{osc}_{[\mathbf{a}, \mathbf{b}]}(f)}{N^{3/4}} \right)^2, \quad (5.13)$$

where $H_1(N, \gamma)$ is given in Eq. (3.9).

Proof. It starts from

$$\mathbb{E}\xi^2 = \frac{2M^2}{N^2} \int_0^{+\infty} u \Pr \left\{ \left| \frac{S_M}{M} - \frac{1}{P} \sum_{i=1}^P f(\mathbf{x}_i) \right| \geq u \right\} du.$$

Owing to the concentration bound (5.5), it further has that

$$\begin{aligned} \mathbb{E}\xi^2 &\leq \frac{4M^2}{N^2} \int_0^{+\infty} u \exp \left(-\frac{2Mu^2}{(1 - M/P)(1 + 1/M)(\text{osc}_{[\mathbf{a}, \mathbf{b}]}(f))^2} \right) du \\ &= \frac{(P - M)(1 + M)}{P} \frac{(\text{osc}_{[\mathbf{a}, \mathbf{b}]}(f))^2}{N^2} \\ &\leq H_1(N, \gamma) \frac{(\text{osc}_{[\mathbf{a}, \mathbf{b}]}(f))^2}{N^{3/2}}. \end{aligned}$$

Since $\mathbb{E}\xi = 0$, it completes the proof. \square

In order to characterize the concentration of the independent sum $\sum_{k=1}^K \xi_k$, we need a basic version of Bernstein's inequality.

Lemma 5 (Bernstein's inequality). *Suppose ξ_k are independent random variables with $|\xi_k| \leq b$, $1 \leq k \leq K$, and $v = \sum_{k=1}^K \mathbb{E}\xi_k^2$. Then for any $\varepsilon \in (0, 1)$, it holds with probability higher than $1 - \varepsilon$ that*

$$\left| \sum_{k=1}^K \xi_k \right| \leq \sqrt{2v \log(2/\varepsilon)} + \frac{2b \log(2/\varepsilon)}{3}. \quad (5.14)$$

Combining Proposition 1, Proposition 2, Proposition 3 and Lemma 5 together finishes the proof of Theorem 2.

Proof of Theorem 2. Since $\mathbb{E}\xi_k = 0$, it has that

$$|\mathbb{E}\mathcal{E}_k(f)| = \left| \frac{1}{N} \frac{M_k}{P_k} \sum_{i=1}^{P_k} f(\mathbf{x}_i) - \frac{1}{N} \frac{M_k}{M_k} \sum_{i=1}^{M_k} f(\mathbf{y}_i) \right| \leq \frac{2\vartheta}{\sqrt{N}} V_{[\mathbf{a}_k, \mathbf{b}_k]}^{HK}(f),$$

the proof of which is the same as that in Eq. (4.9). Combining the above estimate with $|\mathbb{E}\mathcal{E}(f)| \leq \sum_{k=1}^K |\mathbb{E}\mathcal{E}_k(f)|$ recovers Eq. (3.8).

Since $\mathcal{E}_k(f)$ are mutually independent, it has

$$\text{Var}(\mathcal{E}(f)) = \sum_{k=1}^K \text{Var}(\mathcal{E}_k(f)). \quad (5.15)$$

Thus Proposition 3 implies Eq. (3.9) in view of Eq. (3.7).

Finally, setting $v = \text{Var}(\mathcal{E}(f))$ and $b = \max_k \frac{\gamma}{4\sqrt{N}} \text{osc}_{[\mathbf{a}_k, \mathbf{b}_k]}(f)$ in Bernstein's inequality (5.14) directly yields Eq. (3.10). \square

5.2 Variance estimation via bounding discrepancies

We first illustrate concentration bounds of Bernstein's type for the tail probabilities $U_M(\delta)$ and $V_M(\delta)$, see Lemma 6, which uses the local variance

$$\sigma^2 = \frac{1}{P} \sum_{i=1}^P \left(f(\mathbf{x}_i) - \frac{S_P}{P} \right)^2. \quad (5.16)$$

Its detailed proof is omitted and the interested readers can refer to.² Afterwards we will complete the proof of Theorem 3, using the bounds of discrepancies to estimate the local variances and the concentration bounds to estimate the second moment $\mathbb{E}\xi_k^2$.

Lemma 6 (The Bernstein-Serfling inequality). *For $\mathcal{X} = (\mathbf{x}_1, \dots, \mathbf{x}_P) \subset \mathbb{Q}^P$, $\mathbb{Q} = [\mathbf{a}, \mathbf{b}]$, let (X_1, \dots, X_M) be a list of a flexible size $M < P$ sampled without replacement from \mathcal{X} . Then for any $\delta > 0$ and any $\varepsilon \in (0, 1)$, we have*

$$\begin{aligned} U_M(\delta) &\leq 2 \exp \left(\frac{-M\delta^2/2}{\frac{P-M}{P} \left(\frac{M+1}{M} \sigma + \frac{\sqrt{\log(2/\varepsilon^2)(P-M-1)}}{M} \text{osc}_{[\mathbf{a}, \mathbf{b}]}(f) \right) \sigma + \frac{2}{3} \delta \text{osc}_{[\mathbf{a}, \mathbf{b}]}(f)} \right) + 2\varepsilon, \\ V_M(\delta) &\leq 2 \exp \left(\frac{-M\delta^2/2}{\left(\frac{P-M+1}{P} \sigma + \frac{\sqrt{\log(2/\varepsilon^2)(M-1)}}{P} \text{osc}_{[\mathbf{a}, \mathbf{b}]}(f) \right) \sigma + \frac{2}{3} \delta \text{osc}_{[\mathbf{a}, \mathbf{b}]}(f)} \right) + 2\varepsilon. \end{aligned} \quad (5.17)$$

Moreover, it holds with probability higher than $1 - \varepsilon$ that

$$\left| \frac{1}{M} \sum_{t=1}^M f(X_t) - \frac{1}{P} \sum_{i=1}^P f(\mathbf{x}_i) \right| \leq 2\sigma \sqrt{\frac{\rho_M \log(2/\varepsilon)}{M}} + 2 \text{osc}_{[\mathbf{a}, \mathbf{b}]}(f) \left(\frac{\kappa_M \log(2/\varepsilon)}{M} \right), \quad (5.18)$$

where ρ_M is given in Eq. (5.7) and

$$\kappa_M = \begin{cases} \frac{4}{3} + \sqrt{\frac{M}{P} \left(\frac{M-1}{P-M+1} \right)}, & M < P/2, \\ \frac{4}{3} + \sqrt{\left(\frac{P-M-1}{M+1} \right) \left(\frac{P-M}{P} \right)}, & M \geq P/2. \end{cases} \quad (5.19)$$

When $\text{osc}_{[\mathbf{a}, \mathbf{b}]}(f) < \infty$, a trivial bound of the local variance is

$$\sigma^2 = \frac{1}{P} \sum_{i=1}^P \left(\sum_{j=1}^P \frac{f(\mathbf{x}_i) - f(\mathbf{x}_j)}{P} \right)^2 \leq \left(\text{osc}_{[\mathbf{a}, \mathbf{b}]}(f) \right)^2. \quad (5.20)$$

For the points $(\mathbf{x}_1, \dots, \mathbf{x}_P)$ with bounded star discrepancy, we could provide another deterministic bound for σ^2 .

Theorem 4 (A deterministic bound for local variance). *Suppose $\mathcal{X} = (\mathbf{x}_1, \dots, \mathbf{x}_P) \subset \mathbb{Q}^P$ with $\mathbb{Q} = [\mathbf{a}, \mathbf{b}]$ and there is a constant $\delta < P$ such that $D_P^*(\phi(\mathbf{x}_1), \dots, \phi(\mathbf{x}_P)) < \delta/P$, where ϕ is a scaling from $[\mathbf{a}, \mathbf{b}]$ to $[0, 1]^d$. Then we have*

$$\sigma^2 \leq \frac{\delta V_{[\mathbf{a}, \mathbf{b}]}^{HK}(f^2)}{P} + \frac{\delta V_{[\mathbf{a}, \mathbf{b}]}^{HK}(f) \cdot \sup_{[\mathbf{a}, \mathbf{b}]} |f|}{P} + \|f\|_{L^2([\mathbf{a}, \mathbf{b}])} \cdot \text{osc}_{[\mathbf{a}, \mathbf{b}]}(f), \quad (5.21)$$

provided $\text{osc}_{[\mathbf{a}, \mathbf{b}]}(f) < \infty$, $V_{[\mathbf{a}, \mathbf{b}]}^{HK}(f) < \infty$ and $V_{[\mathbf{a}, \mathbf{b}]}^{HK}(f^2) < \infty$.

Proof. Since $\sum_{i=1}^P f(\mathbf{x}_i) = PS_P$, a direct calculation yields that

$$\sigma^2 = \frac{1}{P} \sum_{i=1}^P f^2(\mathbf{x}_i) - \left(\frac{S_P}{P} \right)^2,$$

and then

$$\begin{aligned} \sigma^2 &= \frac{1}{P} \sum_{i=1}^P f^2(\mathbf{x}_i) - \frac{1}{\lambda(\mathbb{Q})} \int_{\mathbb{Q}} f^2(\mathbf{x}) d\mathbf{x} + \frac{1}{\lambda(\mathbb{Q})} \int_{\mathbb{Q}} f^2(\mathbf{x}) d\mathbf{x} - \left(\frac{S_P}{P} \right)^2 \\ &\leq V_{[\mathbf{a}, \mathbf{b}]}^{HK}(f^2) \cdot D_P^*(\phi(\mathbf{x}_1), \dots, \phi(\mathbf{x}_P)) + \frac{1}{\lambda(\mathbb{Q})} \int_{\mathbb{Q}} f^2(\mathbf{x}) d\mathbf{x} - \left(\frac{S_P}{P} \right)^2. \end{aligned}$$

The bounded star discrepancy in the first term gives the first part of the bound

in Eq. (5.21). For the second term, we have that

$$\begin{aligned}
\frac{1}{\lambda(Q)} \int_Q f^2(\mathbf{x}) d\mathbf{x} &= \frac{1}{\lambda(Q)} \int_Q f(\mathbf{x}) \left(f(\mathbf{x}) - \frac{S_P}{P} \right) d\mathbf{x} \\
&\quad + \frac{S_P}{P} \left(\frac{1}{\lambda(Q)} \int_Q f(\mathbf{x}) d\mathbf{x} - \frac{S_P}{P} \right) + \left(\frac{S_P}{P} \right)^2 \\
&\leq \left(\frac{1}{\lambda(Q)} \int_Q f^2(\mathbf{x}) d\mathbf{x} \right)^{1/2} \left(\frac{1}{\lambda(Q)} \int_Q \left(f(\mathbf{x}) - \frac{S_P}{P} \right)^2 d\mathbf{x} \right)^{1/2} \\
&\quad + \frac{\delta V_{[a,b]}^{HK}(f) \cdot \sup_{[a,b]} |f|}{P} + \left(\frac{S_P}{P} \right)^2 \\
&\leq \|f\|_{L^2([a,b])} \cdot \text{osc}_{[a,b]}(f) + \frac{\delta V_{[a,b]}^{HK}(f) \cdot \sup_{[a,b]} |f|}{P} + \left(\frac{S_P}{P} \right)^2,
\end{aligned}$$

which recovers the last two parts of the bound in Eq. (5.21). \square

Combining Theorem 4 with Lemma 6 produces the second stochastic bound for the random variable ξ in Eq. (5.8).

Proposition 4 (The second stochastic bound for random variables). *Suppose $P \geq M > 0$, then for any $\varepsilon \in (0, 1)$, it holds with probability higher than $1 - \varepsilon$ that*

$$|\xi| \leq \sqrt{\log(2/\varepsilon)} \left(\frac{P+1}{N\sqrt{P}} \right) \sigma + \log(2/\varepsilon) \left(\frac{8+3\sqrt{2}}{3N} \right) \text{osc}_{[a,b]}(f), \quad (5.22)$$

provided $\text{osc}_{[a,b]}(f) < \infty$, $V_{[a,b]}^{HK}(f) < \infty$ and $V_{[a,b]}^{HK}(f^2) < \infty$. In particular, when the inequality (5.21) holds for $\delta = \vartheta\sqrt{N}$ and $P \leq \gamma\sqrt{N}$, it holds with probability higher than $1 - \varepsilon$ that

$$|\xi| \leq \frac{3\sqrt{\log(2/\varepsilon)}}{2N^{3/4}} \mathcal{V}_{[a,b]}(f, \vartheta, \gamma) + \frac{(8+3\sqrt{2})\log(2/\varepsilon)}{3N} \text{osc}_{[a,b]}(f), \quad (5.23)$$

where

$$\mathcal{V}_{[a,b]}(f, \vartheta, \gamma) = \sqrt{\vartheta V_{[a,b]}^{HK}(f^2) + \vartheta V_{[a,b]}^{HK}(f) \cdot \sup_{[a,b]} |f| + \gamma \|f\|_{L^2([a,b])} \cdot \text{osc}_{[a,b]}(f)}. \quad (5.24)$$

Proof. When $P = 1$, we have $\kappa_M = 4/3$ and $\rho_M = 0$, with which Eq. (5.22) holds according to Lemma 6. Below we only need to consider $P > 1$.

The first part of the bound in Eq. (5.22) can be readily obtained via applying the fact (5.11) into the first part of the bound in Eq. (5.18).

We have the second part of the bound in Eq. (5.22) from the second part of the bound in Eq. (5.18) if noting

$$\kappa_M \leq \frac{4}{3} + \sqrt{\frac{P-2}{2(P+2)}} \leq \frac{4}{3} + \frac{\sqrt{2}}{2}, \quad (5.25)$$

which can be verified using the fact that the monotonically increasing function $g(x) = \frac{x}{P} \left(\frac{x-1}{P-x+1} \right)$ for $x \in [1, P/2]$ and the monotonically decreasing function $h(x) = \left(\frac{P-x-1}{x+1} \right) \left(\frac{P-x}{P} \right)$ for $x \in [P/2, P]$ both attain the maximal value at $x = P/2$.

Implementing $\delta = \vartheta\sqrt{N}$ and $P \leq \gamma\sqrt{N}$ in Eq. (5.21) yields $\sigma \leq \frac{N^{1/4}}{\sqrt{P}} \mathcal{V}_{[a,b]}(f, \vartheta, \gamma)$, and substituting it into Eq. (5.22) reaches Eq. (5.23). \square

Proposition 5 (The second bound for variance of random matching). *Suppose $P \geq M > 0$, $\text{osc}_{[a,b]}(f) < \infty$ and there exists a constant $\gamma < 1$ such that $P < \gamma\sqrt{N}$. Then*

$$\mathbb{E}\xi^2 \leq \frac{H_2(N)}{N^{1/2}(N+1)} (\mathcal{V}_{[a,b]}(f, \vartheta, \gamma))^2 + \frac{H_3(\gamma, N)}{N(N+1)} \left(\text{osc}_{[a,b]}(f) \right)^2, \quad (5.26)$$

where $H_2(N)$ and $H_3(\gamma, N)$ are given in Eq. (3.11).

Proof. As a convenience, we denote the bound in Eq. (5.23) by

$$B_{\gamma, \vartheta, N}(f) = \frac{C_1}{N^{3/4}} \mathcal{V}_{[a,b]}(f, \vartheta, \gamma) + \frac{C_2}{N} \text{osc}_{[a,b]}(f),$$

where the coefficients C_1 and C_2 both depends on only ε . Then $\Pr(\{|\xi| > B_{\gamma, \vartheta, N}(f)\}) < \varepsilon$, and

$$\mathbb{E}(\xi^2 \cdot \mathbb{1}_{\{|\xi| \leq B_{\gamma, \vartheta, N}(f)\}}) \leq (B_{\gamma, \vartheta, N}(f))^2 (1 - \Pr(\{|\xi| > B_{\gamma, \vartheta, N}(f)\})).$$

On the other hand, the trivial bound in Eq. (5.12) implies

$$\mathbb{E}(\xi^2 \cdot \mathbb{1}_{\{|\xi| > B_{\gamma, \vartheta, N}(f)\}}) \leq \frac{\gamma^2}{16N} \left(\text{osc}_{[a,b]}(f) \right)^2 \Pr(\{|\xi| > B_{\gamma, \vartheta, N}(f)\}).$$

Together, it has for $B_{\gamma, \vartheta, N}(f) \leq \frac{\gamma}{4\sqrt{N}} \text{osc}_{[a,b]}(f)$ that

$$\begin{aligned} \mathbb{E}\xi^2 &= \mathbb{E}(\xi^2 \cdot \mathbb{1}_{\{|\xi| \leq B_{\gamma, \vartheta, N}(f)\}}) + \mathbb{E}(\xi^2 \cdot \mathbb{1}_{\{|\xi| > B_{\gamma, \vartheta, N}(f)\}}) \\ &\leq \left[\frac{\gamma^2}{16N} \left(\text{osc}_{[a,b]}(f) \right)^2 - (B_{\gamma, \vartheta, N}(f))^2 \right] \varepsilon + (B_{\gamma, \vartheta, N}(f))^2 \\ &= (B_{\gamma, \vartheta, N}(f))^2 (1 - \varepsilon) + \frac{\gamma^2 \varepsilon}{16N} \left(\text{osc}_{[a,b]}(f) \right)^2 \\ &\leq \frac{2C_1^2}{N^{3/2}} (\mathcal{V}_{[a,b]}(f, \vartheta, \gamma))^2 (1 - \varepsilon) + \frac{2C_2^2}{N^2} \left(\text{osc}_{[a,b]}(f) \right)^2 (1 - \varepsilon) + \frac{\gamma^2 \varepsilon}{16N} \left(\text{osc}_{[a,b]}(f) \right)^2, \end{aligned}$$

which also holds for $B_{\gamma, \vartheta, N}(f) > \frac{\gamma}{4\sqrt{N}} \text{osc}_{[a,b]}(f)$ due to Eq. (5.12).

Finally, taking $\varepsilon = \frac{1}{N+1}$ recovers Eq. (5.26). \square

The remaining task is to complete the proof of Theorem 3.

Proof of Theorem 3. According to Eqs. (3.7), (5.15) and (5.26), the variance $\text{Var}(\mathcal{E}(f))$ is bounded by

$$\text{Var}(\mathcal{E}(f)) \leq \frac{H_2(N)}{N^{1/2}(N+1)} \sum_{k=1}^K (\mathcal{V}_{[\mathbf{a}_k, \mathbf{b}_k]}(f, \vartheta, \gamma))^2 + \frac{H_3(\gamma, N)}{N(N+1)} \sum_{k=1}^K \left(\text{osc}_{[\mathbf{a}_k, \mathbf{b}_k]}(f) \right)^2.$$

For the first term, we have

$$\begin{aligned} \sum_{k=1}^K (\mathcal{V}_{[\mathbf{a}_k, \mathbf{b}_k]}(f, \vartheta, \gamma))^2 &= \sum_{k=1}^K \vartheta V_{[\mathbf{a}_k, \mathbf{b}_k]}^{HK}(f^2) + \sum_{k=1}^K \vartheta V_{[\mathbf{a}_k, \mathbf{b}_k]}^{HK}(f) \sup_{[\mathbf{a}_k, \mathbf{b}_k]} |f| \\ &\quad + \sum_{k=1}^K \gamma \|f\|_{L^2([\mathbf{a}_k, \mathbf{b}_k])} \text{osc}_{[\mathbf{a}_k, \mathbf{b}_k]}(f) \\ &\leq \vartheta V_{[\mathbf{a}, \mathbf{b}]}^{HK}(f^2) + \vartheta V_{[\mathbf{a}, \mathbf{b}]}^{HK}(f) \sup_{[\mathbf{a}, \mathbf{b}]} |f| + \gamma \sum_{k=1}^K \|f\|_{L^2([\mathbf{a}_k, \mathbf{b}_k])} \text{osc}_{[\mathbf{a}_k, \mathbf{b}_k]}(f). \end{aligned}$$

As a result, it recovers Eq. (3.11). \square

6 Numerical validation

To illustrate the negative particle weights, we consider the numerical integration of a determinantal function

$$I(f) = \int_{\mathbb{R}^d} f(\mathbf{v}) g(\mathbf{v}) d\mathbf{v}, \quad g(\mathbf{v}) = \frac{\det(G(\mathbf{v}))}{\int_{\mathbb{R}^d} \det(G(\mathbf{v})) d\mathbf{v}}, \quad (6.1)$$

the prototypes of which are the Slater-determinant-type wave functions in quantum physics and the determinantal point process, where $G(\mathbf{v}) = (G_{ij}(\mathbf{v}))_{m \times m}$ is a $m \times m$ matrix-valued function with $G_{ij}(\mathbf{v})$ being a function of d variables. Since $g(\mathbf{v})$ is usually not positive semi-definite, the standard Monte Carlo approach is to adopt $|g(\mathbf{v})|$ as the unnormalized instrumental probability density and $w(\mathbf{v}) = g(\mathbf{v})/|g(\mathbf{v})| \in \{-1, 1\}$ as the importance weight as follows

$$I(f) = \mathcal{Z} \int_{\mathbb{R}^d} f(\mathbf{v}) w(\mathbf{v}) \frac{|g(\mathbf{v})|}{\mathcal{Z}} d\mathbf{v}, \quad \mathcal{Z} = \int_{\mathbb{R}^d} |g(\mathbf{v})| d\mathbf{v}.$$

It yields two kinds of estimators $I_+(f)$ and $I_-(f)$:^{23,30}

$$I_+(f) = \mathcal{Z} \left(\frac{\sum_{i=1}^P f(\mathbf{x}_i) w(\mathbf{x}_i) + \sum_{i=1}^M f(\mathbf{y}_i) w(\mathbf{y}_i)}{P + M} \right), \quad (6.2)$$

and

$$I_-(f) = \frac{\sum_{i=1}^P f(\mathbf{x}_i) w(\mathbf{x}_i) + \sum_{i=1}^M f(\mathbf{y}_i) w(\mathbf{y}_i)}{\sum_{i=1}^P w(\mathbf{x}_i) + \sum_{i=1}^M w(\mathbf{y}_i)} = \frac{\sum_{i=1}^P f(\mathbf{x}_i) - \sum_{i=1}^M f(\mathbf{y}_i)}{P - M}, \quad (6.3)$$

where $w(\mathbf{x}_i) = 1$ and $w(\mathbf{y}_i) = -1$. The latter estimator $I_-(f)$ utilizes the strong law of large number

$$\mathcal{Z} \left(\frac{\sum_{i=1}^P w(\mathbf{x}_i) + \sum_{i=1}^M w(\mathbf{y}_i)}{P + M} \right) \rightarrow 1 \quad \text{as } P + M \rightarrow +\infty.$$

Both estimators have the form of Eq. (1.1). In particular, $I_-(f)$ avoids calculating the normalizing constant \mathcal{Z} .

6.1 Experiment setup

We adopt the convention that $\mathbf{v} = (v_1, \dots, v_d) = (\mathbf{v}_1, \dots, \mathbf{v}_m)$ with $n = d/m$, $\mathbf{v}_j = (v_{(j-1)n+1}, \dots, v_{jn}) \in \mathbb{R}^n$, and set

$$G_{ij}(\mathbf{v}) = \begin{cases} \phi_i(\mathbf{v}_i), & i = j, \\ \epsilon \phi_i(\mathbf{v}_j) & i \neq j, \end{cases} \quad (6.4)$$

where $\epsilon \in (0, 1)$ is a parameter and $\phi_i(\mathbf{v}_j)$ ($1 \leq i \leq m, 1 \leq j \leq m$) are given by

$$\phi_i(\mathbf{v}_j) = \frac{1}{(2\pi)^{d/2m}} \exp\left(-\frac{|\mathbf{v}_j - \bar{\mathbf{v}}_i|^2}{2}\right). \quad (6.5)$$

The central positions $\bar{\mathbf{v}}_i \in \mathbb{R}^n$ are composed of $n/3$ integer-valued grid points chosen from the rectangular box $[-4, 5] \times [-2, 3] \times [-2, 3]$.

The positive and negative particles come from the estimator $I_-(f)$ in Eq. (6.3). The relative error

$$\text{r.e.}(f) = \frac{|\mathcal{E}(f)|}{|\int f d\mu|} \quad (6.6)$$

are adopted to evaluate the performance. Below we consider five test functions, denoted by f_1, f_2, f_3, f_4, f_5 . According to Eq. (2.6), the explicit formula for the variation of f_1, f_2, f_5 on $[0, 1]^d$ in the sense of Hardy and Krause can be obtained. One can see that $V_{[0,1]^d}^{HK}(f_1)$ and $V_{[0,1]^d}^{HK}(f_2)$ depend linearly on d , while $V_{[0,1]^d}^{HK}(f_5)$ depends exponentially on d .

- (1) A linear function with vanishing mixed derivatives:

$$f_1(\mathbf{v}) = \sum_{i=1}^d v_i, \quad V_{[0,1]^d}^{HK}(f_1) = \sum_{i=1}^d \int_0^1 dv_i = d. \quad (6.7)$$

- (2) A quadratic function with vanishing mixed derivatives:

$$f_2(\mathbf{v}) = \sum_{i=1}^d v_i^2, \quad V_{[0,1]^d}^{HK}(f_2) = 2 \sum_{i=1}^d \int_0^1 v_i dv_i = d. \quad (6.8)$$

(3) A continuous function with discontinuous derivatives:

$$f_3(\mathbf{v}) = \sum_{i=1}^d |v_i|. \quad (6.9)$$

(4) A continuous function with discontinuous derivatives:

$$f_4(\mathbf{v}) = \max_{1 \leq i \leq d} v_i. \quad (6.10)$$

(5) A continuous function with its variation depending on d exponentially:

$$f_5(\mathbf{v}) = \prod_{i=1}^d v_i, \quad V_{[0,1]^d}^{HK}(f_5) = \sum_{l=1}^d \sum_{F_l} \left(\int_0^1 dv_i \right)^l = 2^d - 1. \quad (6.11)$$

6.2 Implementation

Sampling: The point distributions of $(\mathbf{x}_1, \dots, \mathbf{x}_P)$ and $(\mathbf{y}_1, \dots, \mathbf{y}_M)$ are obtained by the Markov Chain Monte Carlo (MCMC), where a simple Gaussian random walk Metropolis sampling is adopted to draw from $|g(\mathbf{v})|$ with standard deviation 0.1.²³ Under different settings of dimensionality d and rank m , we need to adjust the parameter ϵ to ensure a high acceptance ratio in the Metropolis sampling and avoid the over-repetitions of samples.

Discrepancy: The calculation of the star discrepancy is a NP-hard problem.¹⁰ Nonetheless, it can be realized by an efficient algorithm based on threshold accepting and probabilistic sampling.¹⁰ Here we set the total number of iterations $I = 128$ and the trial time $T = 5$ for each test in order to ensure a satisfactory approximation.

Matching: Two kinds of matching strategies are tested. One is the random matching and the other the optimal assignment. The random matching is realized by sorting a randomly generated sequence in an increasing order. The optimal assignment is realized by the Hungarian algorithm¹⁴ where the distance is chosen as the Manhattan distance. Although the complexity of the Hungarian algorithm scales polynomially in the number of points, its cost still grows dramatically when P_k and M_k become large. Thus for the sake of comparison, we only use the optimal assignment for the experiments of relatively small sample size ($N_{tot} \leq 10^6$).

Parallelization: For each group of experiments, we use 64 threads to generate samples from mutually independent Markov chains and collect all data through Message Passing Interference (MPI) standard. In order to realize the sequential clustering in a distributed platform, we decompose the domain into mutually disjoint 64 bins via balancing the particle numbers in each processor, which in turn strikes a balance in overload. All the numerical examples are obtained with our own Fortran implementations and run on the High-Performance Computing Platform of Peking University with the platform: 2×Intel Xeon E5-2697A v4 (2.60GHz, 40MB Cache, 9.6GT/s QPI Speed, 16 Cores, 32 Threads) and 256GB Memory.

6.3 Numerical results

To clarify the efficiency of SPADE, we calculate the ratio N_{tot}^A/N_{tot} and relative errors for all experiments with $\vartheta = 0.08$ in Table 1, where N_{tot} and N_{tot}^A denote the total particle number before and after annihilation, respectively. The partition levels K and the total wall time in sequential clustering, under different N_{tot} , N , ϑ and d , are collected in Table 2 and Table 3, respectively.

For the readers' convenience, all the raw data, ranging from $d = 12$ to $d = 1080$, are collected in Tables 4-9 in the appendix as supplementary materials. There Rand(1) corresponds to the results obtained by one random matching in each cluster, Rand(100) the averaged results of 100 random matchings, and Hungarian the results produced by the optimal assignment. The parameter ϵ and the acceptance ratio in sampling, the parameter ϑ in adaptive clustering, the positive particle number P , the negative particle number M and the estimators $I_-(f)$ for all test functions are recorded. The results with relative error exceeding 5% are marked in bold font.

Clustering: We first investigate the performance of adaptive clustering. According to Table 2, the partition level K depends on the parameter ϑ , the total sample size N_{tot} and the dimensionality d . By increasing ϑ , it will dramatically reduce the partition level K so that more particles are annihilated. Too small ϑ is not suggested as it will lead to a very large K , resulting in an inefficient annihilation and a severe over-fitting problem (sometimes K even exceeds the total sample size N_{tot}). In addition, we observe that for a fixed ϑ , there is a positive correlation between partition level K and total sample size N_{tot} . In particular, when $\vartheta = 0.08$, K is almost linearly proportional to $\sqrt{N_{tot}}$.

Accuracy and variation: It is readily observed that the accuracy of SPADE is strongly influenced by the variation of test functions. As presented in Table 1, for f_1 , f_2 , f_3 and f_4 , regardless of the continuity of their derivatives, SPADE can achieve a satisfactory accuracy even after removing more than 70% of total particles (see the groups $d = 36$, $N_{tot} = 10^7$, $\vartheta = 0.08$ and $d = 60$, $N_{tot} = 10^7$, $\vartheta = 0.08$). And accurate results are still obtained after removing nearly half of particles in very high dimensional problem (see the group $d = 360$, $N_{tot} = 1 \times 10^7$, $\vartheta = 0.08$). Therefore, for an appropriate class of test functions, SPADE seems to be immune to the curse of dimensionality. By contrast, a severe fluctuation of errors is observed for f_5 , because its total variation depends exponentially on d . This coincides with the predictions of the deterministic bound (3.5) in Theorem 1 and the random bound (3.8) in Theorem 2, as the performances of $\mathcal{E}(f)$ are distinct for different f even under the same sequences before and after annihilation. Nevertheless, the bound provided by (3.5) and (3.8) sometimes turns out to be a gross over-estimate. With an appropriate choice of parameters, SPADE may still be able to preserve the accuracy for test function f_5 in high-dimensional cases after removing more than 10% of total particles (see Table 1 for the groups: $d = 360$, $N_{tot} = 10^5$, $\vartheta = 0.08$, and $d = 1080$, $N_{tot} = 10^6$, $\vartheta = 0.08$).

Matching: We compare the performance of random matching and optimal assignment. With a good partitioning, the accuracy of optimal assignment can be ensured by the deterministic bounds (3.5) in Theorem 1. In general, the optimal

assignment is less accurate than the random matching, especially when d becomes large, because the distance in Euclidian space and its geometric structure are heavily influenced by dimensionality. In contrast, the random matching, regardless of once and many times, can improve the accuracy. This validates the improvement in Eq. (3.8) compared to Eq. (3.5) and the concentration bound (3.10) in Theorem 2. In practice, it suggests to do random matching in each cluster for just once to save the computational time, without loss of accuracy. In fact, the result produced by random matching once is sometimes superior to the average of 100 independent trials.

Computational time: We record the total wall time in second for sequential clustering in Table 3, which occupies more than 90% of total computational time. Three observations are listed as follows. (1) For fixed ϑ and N_{tot} , the total wall time almost increases as d increase. The main reason is that more directions are searched in calculating the star discrepancies.¹⁰ (2) For fixed ϑ and d , the total wall time is almost linearly dependent on the sample size N_{tot} , as well as on the partition level K . This observation is rather important in estimating the computational cost of sequential clustering. (3) For fixed N_{tot} and d , the total wall time in general increases as ϑ is chosen smaller, along with a deeper level of the decision tree. But there are some exceptions. One can see that in the group $d = 1080$, $N_{tot} = 1 \times 10^7$, the computational cost is the highest when $\vartheta = 0.08$, even though the partition level K is the smallest.

7 Conclusion and discussion

We proposed an algorithm, dubbed Sequential-clustering Particle Annihilation via Discrepancy Estimation (SPADE), for efficiently removing particles with opposite weights in an empirical signed measure within an acceptable accuracy. SPADE first seeks adaptive clustering of particles via controlling their number-theoretic discrepancies, then pairs the positive and negative particles via random matching and finally removes the paired ones. It does not require any a priori knowledge of nodal hyper-surface of underlying integrand as adopted in fixed-node approximation, and alleviates the restriction of mesh size in grid-based annihilation, thereby providing a potential approach to overcoming the numerical sign problem in general settings. We have proved that both the deterministic and the random error bounds of SPADE are affected by two factors. One factor measures the irregularity of the point distribution via bounding the star discrepancy in each cluster, and is proportional to n^{-1} (n is the particle number in one cluster). That is, it has the same denominator as the bound of low-discrepancy sequences in quasi-Monte Carlo. Moreover, a unified numerator is set to be $\vartheta\sqrt{N}$ ($\vartheta \in (0, 1)$ is the error-controlling parameter and N is the normalizing constant), thereby avoiding the embarrassing scaling of $(\log n)^d$ in quasi-Monte Carlo (d is the dimensionality). The other factor is the variation of the test function, and implicitly depends on d . Therefore SPADE can be immune to the curse of dimensionality for suitable test functions, which has been validated by numerical experiments up to $d = 1080$.

Table 1: The ratio of annihilation N_{tot}^A/N_{tot} and relative errors $\text{r.e.}(f)$ for random matching ($\vartheta = 0.08$) are presented. Satisfactory results are obtained for test functions f_1 , f_2 , f_3 and f_4 . By contrast, there are a huge fluctuations on the results of f_5 due to its large total variation.

d	N_{tot}	N	N_{tot}^A/N_{tot}	$\text{r.e.}(f_1)$	$\text{r.e.}(f_2)$	$\text{r.e.}(f_3)$	$\text{r.e.}(f_4)$	$\text{r.e.}(f_5)$
12	1×10^4	2446	65.04%	0.2310%	2.4128%	1.1648%	0.9044%	3.1539%
	1×10^5	24836	70.41%	0.6840%	1.6277%	0.8013%	0.9407%	36.8416%
	1×10^6	243326	72.12%	0.5299%	1.6665%	0.8485%	0.9953%	64.5606%
	1×10^7	2403016	75.68%	0.5669%	1.5188%	0.7540%	1.0674%	54.6809%
36	1×10^4	1124	60.64%	1.3238%	3.6452%	1.9537%	0.3123%	202.7732%
	1×10^5	12518	37.76%	1.0242%	3.9932%	2.0902%	1.2407%	5.4367%
	1×10^6	121666	28.21%	0.4692%	3.3817%	1.7842%	1.4046%	128.7225%
	1×10^7	1203984	27.17%	0.0691%	2.7788%	1.4717%	1.0867%	567.4215%
60	1×10^4	260	79.36%	0.2880%	0.5271%	2.0039%	1.7056%	26.8976%
	1×10^5	2760	51.58%	0.4399%	2.4687%	1.0438%	1.1901%	100.6408%
	1×10^6	39256	33.40%	0.9677%	0.1069%	0.3126%	0.5714%	61.8996%
	1×10^7	357952	27.12%	0.6646%	0.7043%	0.1110%	0.4783%	181.1446%
120	1×10^4	138	89.86%	1.3588%	0.3399%	0.2148%	1.1358%	0.0625%
	1×10^5	988	49.27%	1.4231%	1.0547%	0.2036%	1.9710%	3.4353%
	1×10^6	7138	47.44%	1.2049%	2.8825%	1.4231%	0.1650%	100.5381%
	1×10^7	68004	34.53%	0.0959%	2.2392%	1.0184%	0.7300%	87.7581%
360	1×10^4	304	92.26%	0.4972%	0.0593%	0.1184%	0.7640%	6.56E-09
	1×10^5	2768	87.59%	0.2050%	0.0941%	0.0040%	0.3796%	0.0479%
	1×10^6	18604	73.62%	0.0388%	0.0372%	0.0875%	0.2325%	3.4452%
	1×10^7	232048	54.03%	0.0057%	0.2312%	0.0970%	0.1581%	92.0226%
1080	1×10^4	276	90.44%	0.3292%	0.1862%	0.1006%	0.1302%	0.0069%
	1×10^5	3202	86.25%	0.2112%	0.0592%	0.0138%	0.1377%	0.3230%
	1×10^6	31972	88.96%	0.2052%	0.1592%	0.0945%	0.4773%	0.0372%
	1×10^7	182104	91.75%	0.0646%	0.0105%	0.0191%	0.0227%	0.0419%

A direct application of SPADE is to alleviate the exponential growth of both particle number and stochastic variances in simulating classical transport and quantum many-body dynamics, especially those where long-time behaviors of several non-oscillating averaged quantities, or physical observables, are of the most interest. In fact, we have recently employed SPADE to alleviate the numerical sign problem in stochastic Wigner simulations. Numerical results in 6-D phase space are very promising³² and the generalization to 12-D problems is still ongoing.

Table 2: The partition level K in sequential clustering under different total sample size N_{tot} , normalizing constant N , parameter ϑ and d . A positive correlation between K and N_{tot} , and a negative correlation between K and ϑ are observed.

N_{tot}	ϑ	$d = 12$	$d = 36$	$d = 60$	$d = 120$	$d = 360$	$d = 1080$
1×10^4	0.005	11073	12120	12127	12757	13076	12835
	0.02	3886	6160	12127	12757	13076	12835
	0.08	1011	1499	3245	6701	13076	2609
N	–	2446	1124	260	138	304	276
N_{tot}	ϑ	$d = 12$	$d = 36$	$d = 60$	$d = 120$	$d = 360$	$d = 1080$
1×10^5	0.005	61320	117348	122846	134491	140958	145016
	0.02	13472	17249	43761	134367	140958	37940
	0.08	3361	3807	8991	20395	39578	8940
N	–	24836	12518	2760	988	2768	3202
N_{tot}	ϑ	$d = 12$	$d = 36$	$d = 60$	$d = 120$	$d = 360$	$d = 1080$
1×10^6	0.005	180704	265893	467951	1377992	1410399	543961
	0.02	44135	50567	108769	293752	755026	124158
	0.08	11112	11391	20377	55575	153531	30554
N	–	243326	121666	39256	7138	18604	31972
N_{tot}	ϑ	$d = 12$	$d = 36$	$d = 60$	$d = 120$	$d = 360$	$d = 1080$
1×10^7	0.005	569881	738886	1630915	14691077	7969705	3207698
	0.02	146090	159723	318590	3161834	1876241	718666
	0.08	37162	37454	64692	160285	363425	185654
N	–	2403016	1203984	357952	68004	232048	182104

References

- [1] L. L. Baker and N. G. Hadjiconstantinou, Variance reduction for Monte Carlo solutions of the Boltzmann equation, *Physics of Fluids*, 17(2005), 051703.
- [2] R. Bardenet and A. O. Maillard, Concentration inequalities for sampling without replacement, *Bernoulli*, 21(2015), 1361–1385.
- [3] G. Bennett, Probability inequalities for the sum of independent random variables, *Journal of the American Statistical Association*, 57(1962), 33–45.
- [4] G. Booth, A. Thom, and A. Alavi. Fermion Monte Carlo without fixed nodes: A game of life, death, and annihilation in Slater determinant space, *Journal of Chemical Physics*, 131(2009), 054106.
- [5] S. Boucheron, G. Lugosi, and P. Massart, *Concentration Inequalities: A Nonasymptotic Theory of Independence*, Oxford University Press, 2013.

Table 3: The total wall time in second for sequential clustering, which occupies more than 90% of total computational time. The computational time is almost linearly dependent on N_{tot} , and usually increases for a larger d or a smaller ϑ .

N_{tot}	ϑ	$d = 12$	$d = 36$	$d = 60$	$d = 120$	$d = 360$	$d = 1080$
1×10^4	0.005	2.374E-01	6.182E-01	8.029E-01	2.236E+00	4.069E+00	7.544E+00
	0.02	1.341E+02	1.274E+01	8.022E-01	2.044E+00	4.048E+00	7.347E+00
	0.08	2.199E+02	5.184E+02	4.117E+02	2.798E+03	4.267E+00	1.157E+04
1×10^5	0.005	1.581E+03	4.639E+03	6.166E+01	1.172E+02	9.531E+02	8.574E+02
	0.02	1.916E+03	3.542E+03	3.429E+03	7.101E+04	1.099E+03	8.889E+04
	0.08	1.394E+03	3.089E+03	6.313E+03	1.657E+04	5.234E+03	7.225E+04
1×10^6	0.005	1.767E+04	4.799E+04	8.559E+03	1.049E+04	5.127E+04	8.466E+05
	0.02	1.246E+04	3.615E+04	6.357E+04	1.032E+05	2.034E+05	5.816E+05
	0.08	1.145E+04	1.994E+04	3.861E+04	1.170E+05	3.144E+05	6.110E+05
1×10^7	0.005	1.254E+05	3.573E+05	5.225E+05	9.696E+05	1.525E+06	3.784E+06
	0.02	1.060E+05	2.550E+05	5.228E+05	5.742E+05	2.351E+06	3.824E+06
	0.08	9.874E+04	1.725E+05	3.194E+05	7.521E+05	2.455E+06	6.414E+06

- [6] R. E. Caflisch, Monte Carlo and Quasi-Monte Carlo methods, *Acta Numerica*, 7(1998), 1–49.
- [7] Z. Cai, J. Lu, and S. Yang, Inchworm Monte Carlo method for open quantum systems, *Communications on Pure and Applied Mathematics*, available at <https://doi.org/10.1002/cpa.21888>, 2020.
- [8] M. Drmota and R. F. Tichy, *Sequences, Discrepancies and Applications*, Springer, 2006.
- [9] J. L. DuBois, E. W. Brown, and B. J. Alder, Overcoming the fermion sign problem in homogeneous systems, available at https://doi.org/10.1142/9789813209428_0013, 2017.
- [10] M. Gnewuch, M. Wahlstrm, and C. Winzen, A new randomized algorithm to approximate the star discrepancy based on threshold accepting, *SIAM Journal on Numerical Analysis*, 50(2012), 781–807.
- [11] W. Hoeffding, Probability inequalities for sums of bounded random variables, *Journal of the American Statistical Association*, 58(1963), 13–30.
- [12] M. Iazzi, A. A. Soluyanov, and M. Troyer, Topological origin of the fermion sign problem, *Physical Review B*, 93(2016), 115102.
- [13] H. Kosina, M. Nadjalkov, and S. Selberherr, A Monte Carlo method seamlessly linking quantum and classical transport calculations, *Journal of Computational Electronics*, 2(2003), 147–151.

- [14] H. W. Kuhn, The Hungarian method for the assignment problem, *Naval Research Logistics Quarterly*, 2(1955), 83–97.
- [15] L. Kuipers and H. Niederreiter, *Uniform Distribution of Sequences*, Courier Corporation, 2012.
- [16] D. Li, K. Yang, and W. Wong, Density estimation via discrepancy based adaptive sequential partition, *Advances in Neural Information Processing Systems* 29, (2016), 1091–1099.
- [17] L. Lu, H. Jiang, and W. H. Wong, Multivariate density estimation by Bayesian sequential partitioning, *Journal of the American Statistical Association*, 108(2013), 1402–1410.
- [18] H. Niederreiter, Discrepancy and convex programming, *Annali Di Matematica Pura Ed Applicata*, 93(1972), 89–97.
- [19] H. Niederreiter, *Random Number Generation and Quasi-Monte Carlo Methods*, SIAM, 1992.
- [20] A. B. Owen, Multidimensional variation for quasi-Monte Carlo, *Contemporary Multivariate Analysis and Design of Experiments: In Celebration of Professor Kai-Tai Fang’s 65th Birthday*, (2005), 49–74.
- [21] S. Paskov, New methodologies for valuing derivatives, available at <https://www.cs.columbia.edu/technical-reports/#Paskov>, 1996.
- [22] P. J. Reynolds, D. M. Ceperley, B. J. Alder, and W. A. Lester Jr, Fixednode quantum Monte Carlo for molecules, *Journal of Chemical Physics*, 77(1982), 5593–5603.
- [23] C. P. Robert and G. Casella, *Monte Carlo Statistical Methods*, 2nd edition, Springer, New York, 2004,
- [24] R. J. Serfling, Probability inequalities for the sum in sampling without replacement, *Annals of Statistics*, 2(1974), 39–48.
- [25] S. Shao and Y. Xiong, A branching random walk method for many-body Wigner quantum dynamics, *Numerical Mathematics: Theory, Methods and Applications*, 12(2019), 21–71.
- [26] S. Shao and Y. Xiong, Branching random walk solutions to the Wigner equation, available at <https://arxiv.org/abs/1907.01897>, 2019.
- [27] S. Steinerberger, Random restricted matching and lower bounds for combinatorial optimization, *Journal of Combinatorial Optimization*, 24(2012), 280–298.
- [28] V. Todorov, I. Dimov, R. Georgieva, and S. Dimitrov, Adaptive Monte Carlo algorithm for Wigner kernel evaluation, *Neural Computing & Applications*, 4(2019), 1–14.

- [29] I. O. Tolstikhin, Concentration inequalities for samples without replacement, *Theory of Probability & Its Applications*, 61(2017), 462–481.
- [30] M. Troyer and U. J. Wiese, Computational complexity and fundamental limitations to fermionic quantum Monte Carlo simulations, *Physical Review Letter*, 94(2005), 21–71.
- [31] Y. Xiong and S. Shao, The Wigner branching random walk: Efficient implementation and performance evaluation, *Communications in Computational Physics*, 25(2019), 871–910.
- [32] Y. Xiong and S. Shao, The Wigner branching random walk: Overcoming the curse of sign problem, In preparation, 2020.
- [33] B. Yan and R. E. Caflisch, A Monte Carlo method with negative particles for Coulomb collisions, *Journal of Computational Physics*, 298(2015), 711–740.

8 Supplementary: Raw data in numerical experiments

Table 4: Numerical results for $d = 12$, $m = 4$, $\epsilon = 0.6$. Acceptance ratio in MCMC is 85%. The results with relative error exceeding 5% are marked in bold font.

Method	ϑ	K	P	M	$I_-(f_1)$	$I_-(f_2)$	$I_-(f_3)$	$I_-(f_4)$	$I_-(f_5)$
$N_{tot} = P + M = 1 \times 10^4$, $N = P - M = 2446$									
Sample	-	-	6223	3777	3.973E+00	1.616E+01	1.112E+01	2.301E+00	-7.828E-02
	0.005	11073	5675	3229	3.914E+00	1.623E+01	1.112E+01	2.316E+00	-1.176E-01
Rand(1)	0.02	3886	5447	3001	3.945E+00	1.637E+01	1.119E+01	2.315E+00	-1.102E-01
	0.08	1011	4475	2029	3.964E+00	1.655E+01	1.125E+01	2.322E+00	-8.074E-02
	0.005	11073	5675	3229	3.934E+00	1.622E+01	1.113E+01	2.309E+00	-1.167E-01
Rand(100)	0.02	3886	3001	2446	3.923E+00	1.634E+01	1.117E+01	2.314E+00	-1.031E-01
	0.08	1011	4475	2029	3.969E+00	1.653E+01	1.124E+01	2.323E+00	-6.464E-02
	0.005	11073	5675	3229	3.934E+00	1.625E+01	1.113E+01	2.313E+00	-7.326E-02
Hungarian	0.02	3886	3001	2446	3.915E+00	1.637E+01	1.117E+01	2.320E+00	-8.958E-02
	0.08	1011	4475	2029	4.012E+00	1.662E+01	1.127E+01	2.332E+00	-4.762E-02
$N_{tot} = P + M = 1 \times 10^5$, $N = P - M = 24836$									
Sample	-	-	62418	37582	3.956E+00	1.608E+01	1.106E+01	2.279E+00	-1.585E-01
	0.005	61320	58740	33904	3.955E+00	1.611E+01	1.107E+01	2.282E+00	-1.416E-01
Rand(1)	0.02	13472	53684	28848	3.981E+00	1.616E+01	1.108E+01	2.290E+00	-1.283E-01
	0.08	3361	47624	22788	3.983E+00	1.634E+01	1.115E+01	2.301E+00	-1.001E-01
	0.005	61320	58740	33904	3.951E+00	1.609E+01	1.106E+01	2.282E+00	-1.532E-01
Rand(100)	0.02	23532	53684	28848	3.985E+00	1.617E+01	1.109E+01	2.291E+00	-1.392E-01
	0.08	3361	47624	22788	4.007E+00	1.638E+01	1.116E+01	2.303E+00	-8.162E-02
	0.005	61320	58740	33904	3.962E+00	1.610E+01	1.107E+01	2.283E+00	-1.479E-01
Hungarian	0.02	23532	53684	28848	3.989E+00	1.622E+01	1.110E+01	2.296E+00	-1.524E-01
	0.08	3361	47624	22788	4.018E+00	1.637E+01	1.116E+01	2.304E+00	-1.064E-01
$N_{tot} = P + M = 1 \times 10^6$, $N = P - M = 243326$									
Sample	-	-	621663	378337	3.970E+00	1.595E+01	1.102E+01	2.271E+00	-1.352E-02
	0.005	180701	571698	328372	3.968E+00	1.598E+01	1.103E+01	2.276E+00	-1.164E-02
Rand(1)	0.02	44135	530335	287009	3.974E+00	1.606E+01	1.105E+01	2.283E+00	-1.344E-02
	0.08	11112	482285	238959	3.949E+00	1.622E+01	1.112E+01	2.294E+00	-4.791E-03
	0.005	180704	571698	328372	3.966E+00	1.598E+01	1.103E+01	2.276E+00	-1.300E-02
Rand(100)	0.02	44135	530335	287009	3.970E+00	1.605E+01	1.105E+01	2.283E+00	-1.385E-02
	0.08	11112	482285	238959	3.952E+00	1.622E+01	1.112E+01	2.294E+00	1.502E-03
	0.005	180704	571698	328372	3.966E+00	1.598E+01	1.103E+01	2.277E+00	-1.331E-02
Hungarian	0.02	44135	530335	287009	3.972E+00	1.606E+01	1.106E+01	2.284E+00	-2.381E-02
	0.08	11112	482285	238959	3.953E+00	1.621E+01	1.111E+01	2.294E+00	-4.567E-03
$N_{tot} = P + M = 1 \times 10^7$, $N = P - M = 2403016$									
Sample	-	-	6201508	3798492	3.969E+00	1.588E+01	1.101E+01	2.263E+00	1.373E-02
	0.005	569881	5683933	3280917	3.962E+00	1.591E+01	1.101E+01	2.269E+00	1.037E-02
Rand(1)	0.02	146090	5380143	2977127	3.959E+00	1.597E+01	1.103E+01	2.274E+00	1.161E-02
	0.08	37162	4985561	2582545	3.947E+00	1.612E+01	1.109E+01	2.287E+00	6.224E-03
	0.005	569881	5683933	3280917	3.962E+00	1.592E+01	1.102E+01	2.269E+00	1.278E-02
Rand(100)	0.02	146090	5380143	2977127	3.958E+00	1.598E+01	1.103E+01	2.275E+00	9.972E-03
	0.08	37162	4985561	2582545	3.947E+00	1.613E+01	1.109E+01	2.288E+00	6.970E-03

Table 5: Numerical results for $d = 36$, $m = 12$, $\epsilon = 0.3$. Acceptance ratio in MCMC is 75%. The results with relative error exceeding 5% are marked in bold font.

Method	ϑ	K	P	M	$I_-(f_1)$	$I_-(f_2)$	$I_-(f_3)$	$I_-(f_4)$	$I_-(f_5)$
$N_{tot} = P + M = 1 \times 10^4$, $N = P - M = 1124$									
Sample	-	-	5562	4438	2.300E+01	6.681E+01	3.901E+01	3.314E+00	3.793E+01
	0.005	12120	4944	3820	2.335E+01	6.802E+01	3.943E+01	3.341E+00	-3.203E+01
Rand(1)	0.02	6160	4820	3696	2.333E+01	6.760E+01	3.930E+01	3.333E+00	3.764E+01
	0.08	1499	3594	2470	2.330E+01	6.925E+01	3.977E+01	3.324E+00	-3.898E+01
	0.005	12120	4944	3820	2.327E+01	6.758E+01	3.928E+01	3.331E+00	2.524E+01
Rand(100)	0.02	6160	4820	3696	2.335E+01	6.776E+01	3.934E+01	3.333E+00	2.204E+01
	0.08	1499	3594	2470	2.337E+01	6.902E+01	3.973E+01	3.325E+00	-1.649E+01
	0.005	12120	4944	3820	2.342E+01	6.846E+01	3.954E+01	3.349E+00	3.787E+01
Hungarian	0.02	6160	4820	3696	2.349E+01	6.862E+01	3.960E+01	3.350E+00	3.796E+01
	0.08	1499	3594	2470	2.349E+01	6.986E+01	3.997E+01	3.345E+00	-3.794E+01
$N_{tot} = P + M = 1 \times 10^5$, $N = P - M = 12518$									
Sample	-	-	56259	43741	2.361E+01	6.768E+01	3.934E+01	3.293E+00	-8.300E+01
	0.005	117348	50027	37509	2.368E+01	6.820E+01	3.951E+01	3.303E+00	-8.289E+01
Rand(1)	0.02	17249	38458	25940	2.373E+01	6.930E+01	3.986E+01	3.315E+00	-8.098E+01
	0.08	3807	25140	12622	2.385E+01	7.038E+01	4.017E+01	3.334E+00	-8.751E+01
	0.005	117348	50027	37509	2.364E+01	6.817E+01	3.951E+01	3.298E+00	-8.353E+01
Rand(100)	0.02	17249	38458	25940	2.371E+01	6.919E+01	3.983E+01	3.308E+00	-5.103E+01
	0.08	3807	25140	12622	2.390E+01	7.032E+01	4.016E+01	3.331E+00	-3.138E+01
	0.005	117348	50027	37509	2.363E+01	6.840E+01	3.958E+01	3.303E+00	-8.201E+01
Hungarian	0.02	17249	38458	25940	2.372E+01	7.194E+01	4.067E+01	3.362E+00	-8.115E+01
	0.08	3807	25140	12622	2.395E+01	7.179E+01	4.062E+01	3.360E+00	-7.827E+01
$N_{tot} = P + M = 1 \times 10^6$, $N = P - M = 121666$									
Sample	-	-	560833	439167	2.376E+01	6.783E+01	3.941E+01	3.281E+00	2.842E+01
	0.005	265893	424226	302560	2.381E+01	6.870E+01	3.968E+01	3.300E+00	-8.343E-02
Rand(1)	0.02	50567	276064	154398	2.385E+01	6.976E+01	4.000E+01	3.321E+00	-8.660E+00
	0.08	11391	201906	80240	2.387E+01	7.012E+01	4.011E+01	3.328E+00	-8.163E+00
	0.005	265893	424226	302560	2.378E+01	6.868E+01	3.968E+01	3.300E+00	8.456E+00
Rand(100)	0.02	50567	276064	154398	2.382E+01	6.967E+01	3.998E+01	3.319E+00	2.572E+00
	0.08	11391	201906	80240	2.387E+01	7.017E+01	4.012E+01	3.329E+00	-5.450E+00
	0.005	265893	424226	302560	2.378E+01	6.886E+01	3.973E+01	3.303E+00	6.665E+00
Hungarian	0.02	50567	276064	154398	2.380E+01	7.058E+01	4.024E+01	3.343E+00	8.353E+00
	0.08	11391	201906	80240	2.383E+01	7.231E+01	4.075E+01	3.383E+00	-1.907E+01
$N_{tot} = P + M = 1 \times 10^7$, $N = P - M = 1203984$									
Sample	-	-	5601992	4398008	2.387E+01	6.788E+01	3.944E+01	3.285E+00	1.076E+00
	0.005	738886	3302812	2098828	2.390E+01	6.905E+01	3.981E+01	3.307E+00	5.264E+00
Rand(1)	0.02	159723	2419796	1215812	2.391E+01	6.952E+01	3.995E+01	3.316E+00	8.713E+00
	0.08	37454	1960715	756731	2.388E+01	6.977E+01	4.002E+01	3.320E+00	-5.029E+00
	0.005	738886	3302812	2098828	2.390E+01	6.906E+01	3.981E+01	3.307E+00	1.032E+01
Rand(100)	0.02	159723	2419796	1215812	2.390E+01	6.949E+01	3.994E+01	3.314E+00	6.796E+00
	0.08	37454	1960715	756731	2.388E+01	6.977E+01	4.003E+01	3.320E+00	-2.767E+00

Table 6: Numerical results for $d = 60$, $m = 20$, $\epsilon = 0.2$. Acceptance ratio in MCMC is 76%. The results with relative error exceeding 5% are marked in bold font.

Method	ϑ	K	P	M	$I_-(f_1)$	$I_-(f_2)$	$I_-(f_3)$	$I_-(f_4)$	$I_-(f_5)$
$N_{tot} = P + M = 1 \times 10^4$, $N = P - M = 260$									
Sample	-	-	5130	4870	5.858E+01	1.900E+02	8.213E+01	5.174E+00	6.616E+04
	0.005	12127	4572	4312	5.793E+01	1.851E+02	8.054E+01	5.188E+00	2.364E+04
Rand(1)	0.02	12127	4572	4312	5.873E+01	1.859E+02	8.059E+01	5.174E+00	6.714E+04
	0.08	3245	4098	3838	5.875E+01	1.890E+02	8.048E+01	5.262E+00	8.396E+04
	0.005	12127	4572	4312	5.783E+01	1.846E+02	8.046E+01	5.122E+00	6.328E+04
Rand(100)	0.02	12127	4572	4312	5.793E+01	1.843E+02	8.038E+01	5.115E+00	6.691E+04
	0.08	3245	4098	3838	5.880E+01	1.880E+02	8.057E+01	5.133E+00	4.321E+04
	0.005	12127	4572	4312	5.786E+01	1.874E+02	8.095E+01	5.202E+00	6.496E+04
Hungarian	0.02	12127	4572	4312	5.786E+01	1.874E+02	8.095E+01	5.202E+00	6.496E+04
	0.08	3245	4098	3838	5.880E+01	1.912E+02	8.119E+01	5.204E+00	6.776E+04
$N_{tot} = P + M = 1 \times 10^5$, $N = P - M = 2760$									
Sample	-	-	51380	48620	6.119E+01	1.996E+02	8.384E+01	5.162E+00	-3.034E+05
	0.005	122846	45894	43134	6.151E+01	2.022E+02	8.427E+01	5.203E+00	-3.310E+05
Rand(1)	0.02	43761	43277	40517	5.998E+01	2.006E+02	8.392E+01	5.174E+00	-3.015E+05
	0.08	8991	27170	24410	6.145E+01	2.045E+02	8.472E+01	5.224E+00	1.944E+03
	0.005	122846	45894	43134	6.133E+01	2.012E+02	8.413E+01	5.184E+00	-3.233E+05
Rand(100)	0.02	43761	43277	40517	6.147E+01	2.011E+02	8.410E+01	5.174E+00	-3.073E+05
	0.08	8991	27170	24410	6.146E+01	2.042E+02	8.465E+01	5.215E+00	5.232E+03
	0.005	122846	45894	43134	6.109E+01	2.015E+02	8.422E+01	5.194E+00	-3.170E+05
Hungarian	0.02	43761	43277	40517	6.129E+01	2.017E+02	8.422E+01	5.187E+00	-3.135E+05
	0.08	8991	27170	24410	6.172E+01	2.073E+02	8.518E+01	5.269E+00	-1.630E+04
$N_{tot} = P + M = 1 \times 10^6$, $N = P - M = 39256$									
Sample	-	-	519628	480372	6.126E+01	2.039E+02	8.430E+01	5.212E+00	3.763E+05
	0.005	467951	448774	409518	6.116E+01	2.039E+02	8.424E+01	5.213E+00	1.703E+05
Rand(1)	0.02	108769	315699	276443	6.087E+01	2.040E+02	8.420E+01	5.201E+00	2.779E+05
	0.08	20377	186620	147364	6.067E+01	2.037E+02	8.404E+01	5.182E+00	1.434E+05
	0.005	467951	448774	409518	6.116E+01	2.040E+02	8.428E+01	5.208E+00	1.728E+05
Rand(100)	0.02	108769	315699	276443	6.095E+01	2.042E+02	8.426E+01	5.205E+00	1.806E+05
	0.08	20377	186620	147364	6.067E+01	2.039E+02	8.409E+01	5.186E+00	1.512E+05
	0.005	467951	448774	409518	6.112E+01	2.045E+02	8.437E+01	5.216E+00	1.688E+05
Hungarian	0.02	108769	315699	276443	6.086E+01	2.047E+02	8.435E+01	5.207E+00	1.428E+05
	0.08	20377	186620	147364	6.061E+01	2.069E+02	8.471E+01	5.229E+00	9.173E+04
$N_{tot} = P + M = 1 \times 10^7$, $N = P - M = 357952$									
Sample	-	-	5178976	4821024	6.133E+01	2.040E+02	8.419E+01	5.146E+00	5.446E+04
	0.005	1630915	3862236	3504284	6.126E+01	2.050E+02	8.435E+01	5.154E+00	3.798E+03
Rand(1)	0.02	318590	2479225	2121273	6.109E+01	2.057E+02	8.441E+01	5.170E+00	1.482E+04
	0.08	64692	1534956	1177004	6.092E+01	2.054E+02	8.428E+01	5.171E+00	-4.419E+04
	0.005	1630915	3862236	3504284	6.123E+01	2.049E+02	8.435E+01	5.155E+00	2.305E+04
Rand(100)	0.02	318590	2479225	2121273	6.110E+01	2.057E+02	8.442E+01	5.172E+00	7.535E+02
	0.08	64692	1534956	1177004	6.094E+01	2.054E+02	8.428E+01	5.172E+00	-2.793E+04

Table 7: Numerical results for $d = 120$, $m = 40$, $\epsilon = 0.05$. Acceptance ratio in MCMC is 77%. The results with relative error exceeding 5% are marked in bold font.

Method	ϑ	K	P	M	$I_-(f_1)$	$I_-(f_2)$	$I_-(f_3)$	$I_-(f_4)$	$I_-(f_5)$
$N_{tot} = P + M = 1 \times 10^4$, $N = P - M = 138$									
Sample	-	-	5069	4931	5.523E+01	5.269E+02	1.874E+02	6.822E+00	-1.397E+10
	0.005	12757	4602	4464	5.581E+01	5.247E+02	1.869E+02	6.786E+00	-1.397E+10
Rand(1)	0.02	12757	4602	4464	5.586E+01	5.228E+02	1.868E+02	6.736E+00	-1.395E+10
	0.08	6701	4562	4424	5.599E+01	5.287E+02	1.878E+02	6.745E+00	-1.398E+10
	0.005	12757	4602	4464	5.592E+01	5.216E+02	1.863E+02	6.825E+00	-1.398E+10
Rand(100)	0.02	12757	4602	4464	5.606E+01	5.223E+02	1.864E+02	6.822E+00	-1.398E+10
	0.08	6701	4562	4424	5.501E+01	5.207E+02	1.858E+02	6.794E+00	-1.398E+10
	0.005	12757	4602	4464	5.523E+01	5.272E+02	1.878E+02	6.924E+00	-1.395E+10
Hungarian	0.02	12757	4602	4464	5.523E+01	5.272E+02	1.878E+02	6.924E+00	-1.395E+10
	0.08	6701	4562	4424	5.457E+01	5.260E+02	1.875E+02	6.905E+00	-1.395E+10
$N_{tot} = P + M = 1 \times 10^5$, $N = P - M = 988$									
Sample	-	-	50494	49506	5.883E+01	5.123E+02	1.834E+02	6.651E+00	-2.227E+12
	0.005	134491	45961	44973	5.932E+01	5.113E+02	1.833E+02	6.614E+00	-2.213E+12
Rand(1)	0.02	134367	45961	44973	5.912E+01	5.112E+02	1.836E+02	6.615E+00	-2.212E+12
	0.08	20395	36460	35472	5.799E+01	5.069E+02	1.831E+02	6.520E+00	-2.303E+12
	0.005	134491	45961	44973	5.979E+01	5.126E+02	1.837E+02	6.606E+00	-1.964E+12
Rand(100)	0.02	134367	28469	27481	5.980E+01	5.124E+02	1.837E+02	6.613E+00	-2.148E+12
	0.08	20395	36460	35472	5.908E+01	5.082E+02	1.834E+02	6.509E+00	-2.267E+12
	0.005	134491	45961	44973	6.017E+01	5.132E+02	1.836E+02	6.670E+00	-2.212E+12
Hungarian	0.02	134367	28469	27481	6.017E+01	5.132E+02	1.836E+02	6.670E+00	-2.212E+12
	0.08	20395	36460	35472	6.000E+01	5.049E+02	1.825E+02	6.566E+00	-2.302E+12
$N_{tot} = P + M = 1 \times 10^6$, $N = P - M = 7138$									
Sample	-	-	503569	496431	6.020E+01	4.883E+02	1.808E+02	6.334E+00	-1.471E+14
	0.005	1377992	460754	453616	5.970E+01	4.903E+02	1.810E+02	6.350E+00	-1.517E+14
Rand(1)	0.02	293752	405990	398852	6.049E+01	4.999E+02	1.829E+02	6.371E+00	-1.516E+14
	0.08	55575	240772	233634	5.947E+01	5.024E+02	1.834E+02	6.324E+00	7.914E+11
	0.005	1377992	460754	453616	5.934E+01	4.918E+02	1.813E+02	6.371E+00	-1.517E+14
Rand(100)	0.02	293752	405990	398852	6.015E+01	4.984E+02	1.826E+02	6.347E+00	-1.514E+14
	0.08	55575	240772	233634	5.991E+01	5.028E+02	1.837E+02	6.293E+00	1.385E+12
	0.005	1377992	460754	453616	5.885E+01	4.934E+02	1.815E+02	6.380E+00	-1.515E+14
Hungarian	0.02	293752	405990	398852	5.954E+01	4.998E+02	1.828E+02	6.365E+00	-1.511E+14
	0.08	55575	240772	233634	5.931E+01	5.043E+02	1.834E+02	6.342E+00	1.984E+12
$N_{tot} = P + M = 1 \times 10^7$, $N = P - M = 68004$									
Sample	-	-	5034002	4965998	5.873E+01	4.955E+02	1.832E+02	6.331E+00	1.563E+15
	0.005	14691077	4676731	4608727	5.893E+01	4.960E+02	1.834E+02	6.326E+00	1.560E+15
Rand(1)	0.02	3161834	4258819	4190815	5.897E+01	4.975E+02	1.837E+02	6.325E+00	1.551E+15
	0.08	160285	1760628	1692624	5.878E+01	5.066E+02	1.851E+02	6.285E+00	1.914E+14
	0.005	14691077	4676731	4608727	5.889E+01	4.962E+02	1.834E+02	6.329E+00	1.541E+15
Rand(100)	0.02	3161834	4258819	4190815	5.888E+01	4.977E+02	1.837E+02	6.331E+00	1.524E+15
	0.08	160285	1760628	1692624	5.880E+01	5.062E+02	1.851E+02	6.271E+00	1.561E+14

Table 8: Numerical results for $d = 360$, $m = 120$, $\epsilon = 0.02$. Acceptance ratio in MCMC is 63%. The results with relative error exceeding 5% are marked in bold font.

Method	ϑ	K	P	M	$I_-(f_1)$	$I_-(f_2)$	$I_-(f_3)$	$I_-(f_4)$	$I_-(f_5)$
$N_{tot} = P + M = 1 \times 10^4$, $N = P - M = 304$									
Sample	-	-	5152	4848	3.417E+02	2.032E+03	6.813E+02	6.942E+00	1.056E+56
	0.005	13076	4765	4461	3.436E+02	2.031E+03	6.813E+02	6.880E+00	1.056E+56
Rand(1)	0.02	13076	4765	4461	3.438E+02	2.031E+03	6.816E+02	6.911E+00	1.056E+56
	0.08	13076	4765	4461	3.434E+02	2.034E+03	6.821E+02	6.889E+00	1.056E+56
	0.005	13076	4765	4461	3.433E+02	2.030E+03	6.813E+02	6.885E+00	9.825E+55
Rand(100)	0.02	13076	4765	4461	3.434E+02	2.031E+03	6.815E+02	6.885E+00	9.931E+55
	0.08	13076	4765	4461	3.433E+02	2.031E+03	6.815E+02	6.879E+00	9.826E+55
	0.005	13076	4765	4461	3.433E+02	2.030E+03	6.811E+02	6.909E+00	1.056E+56
Hungarian	0.02	13076	4765	4461	3.433E+02	2.030E+03	6.811E+02	6.909E+00	1.056E+56
	0.08	13076	4765	4461	3.433E+02	2.030E+03	6.811E+02	6.909E+00	1.056E+56
$N_{tot} = P + M = 1 \times 10^5$, $N = P - M = 2768$									
Sample	-	-	51384	48616	3.393E+02	1.989E+03	6.734E+02	6.841E+00	-2.897E+56
	0.005	140958	47847	45079	3.391E+02	1.988E+03	6.733E+02	6.842E+00	-2.897E+56
Rand(1)	0.02	140958	47847	45079	3.393E+02	1.990E+03	6.737E+02	6.835E+00	-2.897E+56
	0.08	39578	45178	42410	3.400E+02	1.991E+03	6.734E+02	6.815E+00	-2.895E+56
	0.005	140958	47847	45079	3.389E+02	1.989E+03	6.734E+02	6.835E+00	-2.900E+56
Rand(100)	0.02	140958	47847	45079	3.390E+02	1.990E+03	6.734E+02	6.833E+00	-2.898E+56
	0.08	39578	45178	42410	3.394E+02	1.989E+03	6.731E+02	6.813E+00	-2.905E+56
	0.005	140958	47847	45079	3.392E+02	1.989E+03	6.734E+02	6.830E+00	-2.897E+56
Hungarian	0.02	140958	47847	45079	3.392E+02	1.989E+03	6.734E+02	6.830E+00	-2.897E+56
	0.08	39578	45178	42410	3.395E+02	1.989E+03	6.732E+02	6.810E+00	-2.897E+56
$N_{tot} = P + M = 1 \times 10^6$, $N = P - M = 18604$									
Sample	-	-	509302	490698	3.415E+02	1.997E+03	6.762E+02	6.804E+00	3.128E+59
	0.005	1410399	476948	458344	3.417E+02	1.998E+03	6.764E+02	6.797E+00	3.128E+59
Rand(1)	0.02	755026	474596	455992	3.415E+02	1.997E+03	6.762E+02	6.797E+00	3.128E+59
	0.08	153531	377425	358821	3.417E+02	1.996E+03	6.756E+02	6.788E+00	3.020E+59
	0.005	1410399	476948	458344	3.417E+02	1.998E+03	6.764E+02	6.800E+00	3.115E+59
Rand(100)	0.02	755026	474596	455992	3.417E+02	1.998E+03	6.763E+02	6.798E+00	3.117E+59
	0.08	153531	377425	358821	3.415E+02	1.996E+03	6.756E+02	6.785E+00	3.004E+59
	0.005	1410399	476948	458344	3.418E+02	1.998E+03	6.764E+02	6.802E+00	3.037E+59
Hungarian	0.02	755026	474596	455992	3.418E+02	1.998E+03	6.763E+02	6.800E+00	3.037E+59
	0.08	153531	377425	358821	3.416E+02	1.996E+03	6.757E+02	6.791E+00	3.021E+59
$N_{tot} = P + M = 1 \times 10^7$, $N = P - M = 232048$									
Sample	-	-	5116024	4883976	3.405E+02	1.987E+03	6.735E+02	6.768E+00	1.651E+60
	0.005	7969705	4851894	4619846	3.405E+02	1.988E+03	6.737E+02	6.767E+00	1.646E+60
Rand(1)	0.02	1876241	4231671	3999623	3.405E+02	1.989E+03	6.739E+02	6.757E+00	1.637E+60
	0.08	363425	2817699	2585651	3.405E+02	1.992E+03	6.742E+02	6.757E+00	1.317E+59
	0.005	7969705	4851894	4619846	3.405E+02	1.988E+03	6.737E+02	6.766E+00	1.639E+60
Rand(100)	0.02	1876241	4231671	3999623	3.404E+02	1.989E+03	6.739E+02	6.758E+00	1.632E+60
	0.08	363425	2817699	2585651	3.404E+02	1.992E+03	6.742E+02	6.757E+00	1.946E+59

Table 9: Numerical results for $d = 1080$, $m = 120$, $\epsilon = 0.02$. Acceptance ratio in MCMC is 63%. The results with relative error exceeding 5% are marked in bold font.

Method	ϑ	K	P	M	$I_-(f_1)$	$I_-(f_2)$	$I_-(f_3)$	$I_-(f_4)$	$I_-(f_5)$
$N_{tot} = P + M = 1 \times 10^4$, $N = P - M = 276$									
Sample	-	-	5262	4722	5.296E+02	6.366E+03	2.149E+03	7.026E+00	-3.207E+189
	0.005	12835	5026	4486	5.295E+02	6.369E+03	2.150E+03	7.029E+00	-3.207E+189
Rand(1)	0.02	12835	5026	4486	5.292E+02	6.373E+03	2.151E+03	7.022E+00	-3.207E+189
	0.08	2609	4792	4252	5.314E+02	6.377E+03	2.151E+03	7.035E+00	-3.206E+189
	0.005	12835	5026	4486	5.299E+02	6.370E+03	2.150E+03	7.028E+00	-3.207E+189
Rand(100)	0.02	12835	5026	4486	5.299E+02	6.370E+03	2.150E+03	7.030E+00	-3.207E+189
	0.08	2609	4792	4252	5.318E+02	6.373E+03	2.151E+03	7.053E+00	-3.206E+189
	0.005	12835	5026	4486	5.292E+02	6.370E+03	2.150E+03	7.021E+00	-3.207E+189
Hungarian	0.02	12835	5026	4486	5.292E+02	6.370E+03	2.150E+03	7.021E+00	-3.207E+189
	0.08	2609	4792	4252	5.311E+02	6.375E+03	2.151E+03	7.036E+00	-3.206E+189
$N_{tot} = P + M = 1 \times 10^5$, $N = P - M = 3202$									
Sample	-	-	52782	47218	5.289E+02	6.364E+03	2.148E+03	6.996E+00	-6.283E+193
	0.005	145016	51905	46341	5.293E+02	6.363E+03	2.148E+03	7.001E+00	-6.283E+193
Rand(1)	0.02	37940	51515	45951	5.296E+02	6.362E+03	2.148E+03	6.993E+00	-6.283E+193
	0.08	8940	45909	40345	5.300E+02	6.360E+03	2.148E+03	7.005E+00	-6.262E+193
	0.005	145016	51905	46341	5.294E+02	6.364E+03	2.148E+03	6.996E+00	-6.283E+193
Rand(100)	0.02	37940	51515	45951	5.295E+02	6.362E+03	2.148E+03	6.994E+00	-6.271E+193
	0.08	8940	45909	40345	5.303E+02	6.360E+03	2.148E+03	7.004E+00	-6.266E+193
	0.005	145016	51905	46341	5.292E+02	6.364E+03	2.148E+03	6.996E+00	-6.283E+193
Hungarian	0.02	37940	51515	45951	5.293E+02	6.362E+03	2.148E+03	6.995E+00	-6.283E+193
	0.08	8940	45909	40345	5.302E+02	6.362E+03	2.148E+03	7.006E+00	-6.262E+193
$N_{tot} = P + M = 1 \times 10^6$, $N = P - M = 31972$									
Sample	-	-	527822	472178	5.286E+02	6.364E+03	2.148E+03	6.997E+00	7.041E+195
	0.005	543961	525331	469687	5.287E+02	6.364E+03	2.148E+03	6.999E+00	7.041E+195
Rand(1)	0.02	124158	517840	462196	5.288E+02	6.366E+03	2.149E+03	7.006E+00	7.041E+195
	0.08	30554	472631	416987	5.297E+02	6.374E+03	2.150E+03	7.031E+00	7.044E+195
	0.005	543961	525331	469687	5.287E+02	6.364E+03	2.148E+03	6.999E+00	7.041E+195
Rand(100)	0.02	124158	517840	462196	5.288E+02	6.366E+03	2.149E+03	7.006E+00	7.041E+195
	0.08	30554	472631	416987	5.297E+02	6.374E+03	2.150E+03	7.031E+00	8.807E+195
	0.005	543961	525331	469687	5.286E+02	6.364E+03	2.148E+03	6.999E+00	7.041E+195
Hungarian	0.02	124158	517840	462196	5.287E+02	6.366E+03	2.148E+03	7.006E+00	7.041E+195
	0.08	30554	472631	416987	5.296E+02	6.372E+03	2.150E+03	7.033E+00	9.248E+195
$N_{tot} = P + M = 1 \times 10^7$, $N = P - M = 182104$									
Sample	-	-	5858055	4141945	5.351E+02	6.427E+03	2.160E+03	7.157E+00	4.825E+198
	0.005	3207698	5843127	4127017	5.351E+02	6.427E+03	2.160E+03	7.157E+00	4.826E+198
Rand(1)	0.02	718666	5790453	4074343	5.351E+02	6.427E+03	2.160E+03	7.157E+00	4.824E+198
	0.08	185654	5445547	3729437	5.354E+02	6.427E+03	2.160E+03	7.158E+00	4.827E+198
	0.005	3207698	5843127	4127017	5.351E+02	6.427E+03	2.160E+03	7.157E+00	4.825E+198
Rand(100)	0.02	718666	5790453	4074343	5.351E+02	6.427E+03	2.160E+03	7.157E+00	4.824E+198
	0.08	185654	5445547	3729437	5.354E+02	6.427E+03	2.160E+03	7.158E+00	4.826E+198